202
4/21/70
C

1333

USNRDL-TR-69-75
WASH 1151
JUNE 1969

IMPLICATIONS OF SUBSTITUTION OF STRONTIUM OXIDE FOR STRONTIUM TITANATE IN TERRESTRIAL/MARINE RADIOISOTOPIC POWER UNITS

PREPARED BY

NAVAL RADIOLOGICAL DEFENSE LABORATORY

SAN FRANCISCO CALIFORNIA 94135

P5009

FOR

U. S. ATOMIC ENERGY COMMISSION

DISCLAIMER

LEGAL NOTICE

This book was prepared under the sponsorship of the U. S. Atomic Energy Commission. Neither the United States, nor the Commission, nor any person acting on behalf of the Commission:

A. Makes any warranty or representation, expressed or implied, with respect to the accuracy, completeness, or usefulness of the information contained in this publication or that the use of any information, apparatus, method, or process disclosed in this book may not infringe privately owned rights; or

B. Assumes any liabilities with respect to the use of, or for damages resulting from the use of any information, apparatus, method, or process disclosed in this publication.

As used in the above, "person acting on behalf of the Commission" includes any employee or contractor of the Commission, or employee of such contractor, to the extent that such employee or contractor of the Commission, or employee of such contractor prepares, disseminates, or provides access to, any information pursuant to his employment or contract with the Commission, or his employment with such contractor.

For sale by the Superintendent of Documents, U.S. Government Printing Office
Washington, D.C., 20402 - Price $1

AUTHORS: S. Z. Mikhail, L. R. James

ABSTRACT

Comparison is made between the principal physical-chemical characteristics of strontium-90 oxide and strontium-90 titanate. Weights of component materials were compared for two 60 W(e) radioisotopic generators each employing one of the two different strontium fuels. Exposure modes that may accidentally occur during transport, implantment or usage of the generators are examined and relative hazards estimated for each mode.

A three dimensional ocean diffusion model is discussed and digital computer codes for both an instantaneous and a continuous fuel release are described. Results of a parametric study showing the effect of varying the empirical constants of the diffusion model are presented.

The biological implications of an accidental release of strontium-90 oxide in the ocean are summarized. This summary includes a description of a migratory marine organism contamination model along with calculated results.

SUMMARY

The Problem

Strontium-90 oxide is an appealing substitution for strontium-90 titanate as fuel for radioisotopic generators because of its higher specific power. Since it is a strong beta-emitting "boneseeker" strontium-90 is one of the more hazardous radioelements. It is essential to evaluate the safety of using the soluble strontium-90 oxide instead of the relatively insoluble titanate. One of the major concerns in assessing the potential hazard of a fuel release is the transport of dissolved fuel in an ocean environment and its biological implications.

The Findings

Each of the oxide and titanate forms has respective advantages as radioisotopic fuel. Using the oxide form results in typical savings of 20% in construction materials of a power system. An oxide fuel capsule, if intact, delivers doses higher by a factor of 1.06 to 1.5 than an equivalent titanate capsule. In case of accidental fuel release in the form of fine powder, doses from the oxide particles would be higher by a factor of about 1.6 than titanate particles of equal size. When deposited in a human gastrointestinal tract the oxide dissolves fast and subjects the bone to a 1.6-72 times higher doses than the titanate. Titanate particles settling on the GI epithelial lining for a few hours could deliver doses in excess of the maximum allowable yearly dose but to a limited area of tissue. Amounts of strontium-90 translocated to the different body organs after deposition in the deep lung are in the case of titanate particles about 56% of those from oxide particles of the same size. Titanate particles, however, expose the lung to about 0.2 rems while dissolving.

Results describing the instantaneous release of strontium-90 oxide and the continuous release of strontium-90 titanate into an ocean environment were obtained from a modified version of the three dimensional Carter-Okubo diffusion model. These results included calculations of contaminated volume, ellipsoid dimensions, amount of radioactivity, and duration of the radioactive pool. A parametric study showing the effect of varying the empirical constants in the diffusion model was also made.

The results from the ocean diffusion model were then used in a migratory marine organism contamination model to predict the level of contamination among certain important marine organisms in California coastal waters. The limitations of the migratory marine model and

possible exposure of marine organisms which are not covered by the model are discussed.

The report assesses the potential hazards from an accidental fuel release into the ocean environment. The following general conclusions were drawn:

1. An instantaneous strontium-90-oxide release would result in a relatively large contaminated pool which would last for a relatively short period of time while a continuous strontium-90-titanate release would produce a much smaller pool which would last for a much longer period of time.

2. Although the empirical diffusion model parameters affect the dimensions and the duration of the radioactive pool, the effect of these parameters on the migratory marine organism contamination model was relatively small.

3. The instantaneous release from a 500 watt(e) strontium-90 oxide source would result in radiocontamination levels in the migratory fish which are negligibly small when compared to the water contamination levels.

TABLE OF CONTENTS

TABLE OF CONTENTS - (Cont'd)

LIST OF TABLES

LIST OF FIGURES

INTRODUCTION

Despite the fact that there are over 600 naturally occurring or artificially produced radioisotopes, surprisingly only a few possess properties suitable for use as a heat source. Three nuclides used in currently operating radioisotopic energy generators (SNAP units) are ^{90}Sr, ^{210}Po and ^{238}Pu. In addition, approximately 17 other isotopes have been considered. Strontium-90 in the form of $SrTiO_3$ has been used successfully as a source of heat in the following radioisotopic generators:[1] Sentry, SNAP 7A, B, C, D, E, & F; 17A, B; 21; 23; RIPPLE Ia&b; IIa&b, Milliwatt 3000, LCG-25 A&B, AGN (URIPS) and AI (3 watt). Strontium-90 oxide, on the other hand, has previously been utilized only in the NUMEC units operated outside of the U.S. for terrestrial application. The essential characteristics of these generators are given in Appendix A.

Due to the higher specific power of ^{90}SrO relative to $^{90}SrTiO_3$,* substitution of the oxide for the titanate as the fuel in future marine/terrestrial SNAP devices can potentially produce higher efficiency in thermal to electrical energy conversion. In addition convenience in design of the generators and savings in construction materials also favor ^{90}SrO.

Since it is a strong β-emitting "boneseeker", ^{90}Sr is one of the more hazardous radioelements. Therefore, it is quite important to evaluate the safety of using the soluble strontium-90 oxide instead of the relatively insoluble titanate.

*See Appendix B for fuel characteristics

In assessing the potential hazards of fuel release the environment in which the radioisotopic unit will be used should be considered. For marine units in transit and for the terrestrial unit, accidental release of the fuel capsule may overexpose personnel. The other conceivable but highly improbable mode of fuel release is the leakage of fuel aerosol through a crack developed in the capsule as a result of external heating in a sustained fire. Hazard comparison in this case will be limited to evaluation of the ratio of doses delivered to the lung, bone, and gastrointestinal tract as a result of inhalation and ingestion of the fine aerosol particulates.

The report begins with a qualitative comparison between the principal physico-chemical characteristics of SrO and $SrTiO_3$ of considerable importance in SNAP unit development. Details of those characteristics are included in Appendix B.

In Section II the weights of component materials are compared for two radioisotopic generators each employing one of the two different strontium fuels. A hypothetical generator was chosen containing the typical components found in SNAP-23. Calculations were based upon directly usable information from the SNAP-23 reports by Westinghouse Astronuclear Laboratory (WANL).

Section III discusses the exposure modes and develops in detail the mathematical models used in investigating transport of the dissolved fuel in the ocean. A three-dimensional Ocean Turbulent Diffusion model devised by Carter & Okubo[3] and further developed and programmed by NRDL[4] describes: (1) the temporal and spacial radionuclide concentration dependence in ocean water; (2) the volume of water within a given concentration contour at any given time; (3) a time-averaged volume within which the radionuclide concentration is equal to or exceeds a pre-specified level; and (4) the total activity inventory within any concentration envelope. Vaughan et al[2] used these results to evaluate the radiological implications of the fuel release. Section IV presents Vaughan's major findings and conclusions in an abbreviated form.

I. COMPARISON OF THE MAIN CHARACTERISTICS OF STRONTIUM-90 OXIDE AND STRONTIUM-90 TITANATE

Inasmuch as the two fuel forms of interest are compounds containing the same radioactive isotope, the properties that lend themselves to comparison are the thermal, mechanical and some of the physical features. Data accumulated from the open literature as well as Oak Ridge National Laboratory sources appear in Appendix B. Table 1 summarizes the most pertinent information and qualitatively compares the physical and chemical characteristics of interest.

TABLE 1

COMPARISON OF PHYSICAL AND CHEMICAL CHARACTERISTICS OF STRONTIUM-90 OXIDE AND STRONTIUM-90 TITANATE

Property	$SrTiO_3$	SrO
Thermal Stability	Both favorable at operating temperatures encountered in marine and terrestrial devices	⟶
Solubility in Seawater	Very low solubility rate for fuel pellet sizes typical of SNAP units	Rapid reaction with water for all fuel pellet sizes typical of SNAP units
Compatibility with Encapsulants		
a. Haynes 25	More favorable	Less favorable
b. Molybdenum	Equally favorable	⟶
c. Tungsten	Less favorable	More favorable
d. Nionel	More favorable	Less
e. TZM	Equally favorable	⟶
Specific Power	0.232 watt/g	0.417 watt/g
Volume per watt (t)	0.86 cm^3	0.52 cm^3
Thermal Conductivity	Much more favorable	Much less favorable

From Table 1 it is apparent that both $^{90}SrTiO_3$ and ^{90}SrO have respective advantages as fuels. Their physicochemical characteristics alone cannot, therefore, serve as a basis for preference of one over the other.

II. MATERIALS SAVINGS

An additional criteria to consider in choosing one fuel form is provided by calculating the weights of component materials required to construct generators of the same thermal output employing the two different fuel forms ($SrTiO_3$ and SrO). Although this criterion is not of utmost importance, it does merit consideration. The savings acquired by utilizing the oxide as fuel depend on the particular radioisotopic thermal generator (RTG) design considered. Furthermore, the design of a SrO-fueled generator if optimized for thermal-to-electric conversion efficiency will be different from that of a $SrTiO_3$-fueled generator of the same power output. Hence, a precise calculation of savings is impossible unless the detailed optimized designs of both generators are available. An estimate of the savings was obtained by choosing a hypothetical 60 watt generator containing the typical components found in SNAP-21 and SNAP-23 systems. Figure 1 is a sketch of such a model, showing the materials used and their dimensions. Table 2 lists the dimensions used for the material weight calculations. The dimensions shown in Table 2 for the $SrTiO_3$ system had been selected for parametric shielding studies by WANL[5] as a part of the SNAP-23 development program. The graphical display obtained in the WANL work was needed to provide shielding and insulation data for this comparative study.

Several assumptions have been made and are listed below:

(1) For $^{90}SrTiO_3$, 4 inch diameter fuel pellets were chosen. WANL determined this diameter to be the best compromise between present engineering capabilities and weight reduction of the RTG[6] system.

(2) The length to diameter ratio necessary to produce 60 watts (e) for ^{90}SrO fuel will be the same as that of the $^{90}SrTiO_3$ fuel. In accordance with the WANL parametric shielding data[7] such ratio was chosen as 1.722.

(3) Thickness of the shielding may be minimized at the expense of more insulation because this minimizes the total weight of the system.[8]

(4) The amount of shielding is such that the exposure dose rate at the surface is 200 mrad/hr or 10 mrad hr 100 cm away from the surface, whichever is greater.

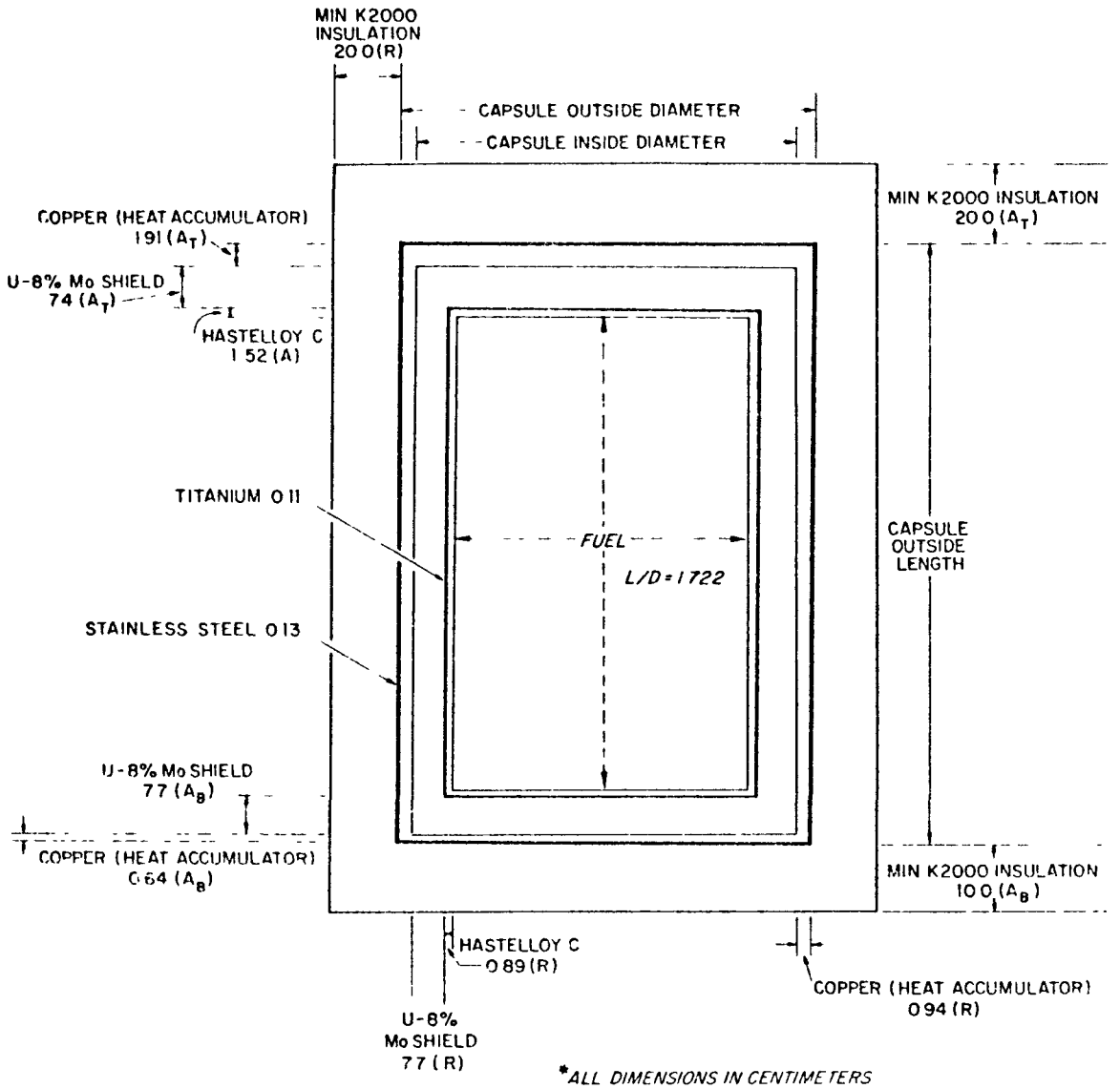

*ALL DIMENSIONS IN CENTIMETERS
(R) APPLIES TO THICKNESS IN RADIAL DIRECTION
(A_T) APPLIES TO THICKNESS IN AXIAL TOP DIMENSION
(A_B) APPLIES TO THICKNESS IN AXIAL BOTTOM DIMENSION
ABSENCE OF EXPLANATORY LETTER MEANS THICKNESS IS THE SAME IN ALL DIRECTIONS

† NUMERICAL VALUES FROM PHASE I, QUARTERLY PROGRESS REPORT WANL-PR-(SS)-004, MARCH 1 - MAY 31, 1967, WESTINGHOUSE ASTRONUCLEAR LAB, p 3-114

Figure 1. Model of a 60 W(e) Radioisotopic Generator

TABLE 2

DIMENSIONS OF 60-WATT(e) ^{90}SrO AND $^{90}SrTiO_3$ CAPSULES*

Material	Dimensions (cm)					
	$SrTiO_3$*			SrO		
	ID	OD	OL	ID	OD	OL
Fuel	10.16		17.50	8.58		14.79
Hastelloy C	10.16	11.94	20.54	8.58	10.36	17.83
Titanium	11.94	12.16	20.76	10.36	10.58	18.05
Shielding	12.16	27.56	35.86	10.58	25.98	33.15
Copper	27.56	29.44	38.41	25.98	27.86	35.70
Stainless Steel	29.44	29.70	38.67	27.86	28.12	35.96
Insulation	29.70	69.70	68.67	28.12	68.12	65.96

*Reference 5

(5) The different volumes of $SrTiO_3$ and SrO require the same thickness of shielding and insulation. Such an assumption will give the maximum difference in weight between a $SrTiO_3$ fueled, and a SrO fueled generator. Arnold's[9] data show an average ratio of 1.04 between the uranium shield needed for a SrO source and that needed for a $SrTiO_3$ source of the same power if the exposure dose is 10 mrem/hr, 100 cm away from the surface. The following values are interpolations from his curves.

Source Power in Watts	Shield Thickness, Cm							
	100 W	200 W	500 W	1000 W	2000 W	5000 W	10,000 W	20,000 W
SrO	6.4	7.0	7.7	8.3	8.8	9.5	9.9	10.25
$SrTiO_3$	6.2	6.7	7.4	7.95	8.4	9.15	9.4	9.8
Ratio	1.03	1.04	1.04	1.04	1.05	1.04	1.05	1.04

(6) A power output level of 60 watts (e) [1200 watts (t)] was chosen because more parametric shielding studies were available for this level than alternative levels.

Table 3 compares the volumes of materials required for the $SrTiO_3$ and SrO fueled generators. Table 4, in analogous fashion, compares the component weights. The savings in replacing the titanate with an oxide heat source appear to be approximately 20% on the average.

III. SAFETY EVALUATION

Comparison between safety aspects of ^{90}SrO and $^{90}SrTiO_3$-fueled sources can be made by examining the exposure modes expected to occur if their corresponding fuels were accidentally released and estimating the relative potential injury to man. This study will not analyze each conceivable hazard situation in detail. Such analyses are normally covered in safety analysis reports written specifically for each radioisotopic generator. The discussion here will be limited to the aspects of analysis necessary to establish a basis for comparing the relative hazards of the two fuels.

TABLE 3

VOLUMETRIC COMPARISON OF 60-WATT(e) CAPSULES

Material	Density (g/cc)	$SrTiO_3$ Fuel - Volume* (cm^3)					SrO Fuel - Volume (cm^3)				
		(R)	(A)				(R)	(A)			
Hastelloy C	8.94	540.7	+ 340.4	=		881.1	391.4	+ 256.1	=		647.5
		(R)	(A)				(R)	(A)			
Titanium	4.5	85.62	+ 25.54	=		111.16	64.52	+ 19.33	=		83.85
		(R)	(A_T)	(A_B)			(R)	(A_T)	(A_B)		
Shielding	17.4	9968.3	+ 4412.2	+ 4591.1	=	18971.6	7977.6	+ 3920.8	+ 4079.8	=	15,978.2
		(R)	(A_T)	(A_B)			(R)	(A_T)	(A_B)		
Copper	8.9	3016.6	+ 1299.5	+ 435.4	=	4751.5	2634.0	+ 1163.8	+ 390.0	=	4187.8
		(R)	(A)				(R)	(A)			
Stainless Steel	8.16	463.7	+ 180.0	=		643.8	407.8	+ 161.4	=		569.2
		(R)	(A_T)	(A_B)			(R)	(A_T)	(A_B)		
Insulation	0.32	120,695	+ 76,272	+ 38,136	=	234,701	108,669	+ 72,853	+ 36,427	=	217,949

*(R) - Radial; (A) - Axial; (A_T) - Axial, Top; (A_B) - Axial, Bottom

TABLE 4

MASS COMPARISON OF 60-WATT(e) CAPSULES

Material	$SrTiO_3$ Mass, kg	$SrTiO_3$ Mass, lb	SrO Mass, kg	SrO Mass, lb	Weight, SrO / Weight, $SrTiO_3$ X 100 Capsule
Hastelloy C	7.88	17.37	5.79	12.76	73.4%
Titanium	0.500	1.103	0.377	0.832	75.4
Shielding	330.12	727.88	278.0	613.0	84.2
Copper	42.29	93.25	37.27	82.18	88.1
Stainless Steel	5.25	11.58	4.64	10.24	88.3
Insulation	75.10	165.61	69.74	153.8	92.8

Credible accidents resulting in hazards may occur during assembly, transporation, implantment or operation of a terrestrial/marine radioisotopic unit. Accidents during assembly can be considered negligible because proper safety precautions can be taken to effectively prevent their occurrence. Accidents during truck or airplane transportation where severe impact and/or fire takes place could lead (although with an extremely small probability) to one of the following situations:

a) Overexposure of personnel resulting from accidental release of the intact fuel capsule from the generator.

b) Eventual fuel release into air or seawater after ground or sea burial of the fuel capsule.

c) Rupture or meltdown of the fuel capsule and release of some of the fuel to the atmosphere.

Implantation of a terrestrial unit is not expected to cause any adverse predicament beyond the release of an intact fuel capsule even under the most severe conditions. On the other hand, implantation of a marine unit may result in burial of the capsule in ocean bottom material which could subsequently release some of the fuel to sea water.

Hazards predicted from operation of a terrestrial unit should not exceed an accidental overexposure of personnel from an intact source; in the case of severe fire there may be a very limited probability of inhalation exposure from fuel release to the atmosphere. Most fuel capsules are designed to stand temperatures up to 2200°F. Such temperatures are attained in fires of fossil fuels.

This brief discussion of the exposure modes to ^{90}SrO and $^{90}SrTiO_3$ sources indicates three situations should be considered: (1) irradiation from an intact capsule; (2) exposure to fuel released into the atmosphere; and (3) exposure of marine organisms to fuel released into seawater.

III.1 Intact Fuel Capsule

Interpolation of Arnold's bremsstrahlung dose rate curves from unshielded isotopic sources of ^{90}SrO and $^{90}SrTiO_3$ as a function of distance from source center yielded the data in Table 5. The data show that overexposure from a ^{90}SrO capsule would be 1.06 to 1.5 times higher than overexposure from a $^{90}SrTiO_3$ capsule of the same thermal output. The data in Table 5 also reveal that the ratio of the doses delivered by equivalent oxide and titanate sources varies as the source power increases. This is obviously due to the higher bremsstrahlung attenuation in the bulkier titanate sources.

TABLE 5

COMPARISON BETWEEN BREMSSTRAHLUNG DOSE RATES FROM UNSHIELDED ISOTOPIC SOURCES OF ^{90}SrO AND $^{90}SrTiO_3$

	Dose Rates (Rads/hr) and Dose Rate Ratios At									
	1 M	2 M	3 M	4 M	5 M	6 M	7 M	8 M	9 M	10 M
100 W, Oxide	1.8×10^{5}	4.5×10^{4}	2.0×10^{4}	1.2×10^{4}	7.2×10^{3}	5.1×10^{3}	3.8×10^{3}	2.9×10^{3}	2.2×10^{3}	1.8×10^{3}
100 W, Titanate	1.7×10^{5}	4.1×10^{4}	1.8×10^{4}	9.7×10^{3}	6.2×10^{3}	4.4×10^{3}	3.3×10^{3}	2.6×10^{3}	1.9×10^{3}	1.7×10^{3}
Ratio	1.06	1.10	1.11	1.24	1.16	1.16	1.15	1.12	1.13	1.06
200 W, Oxide	3.7×10^{5}	9.0×10^{4}	4.0×10^{4}	2.3×10^{4}	1.6×10^{4}	1.0×10^{4}	7.6×10^{3}	5.8×10^{3}	4.6×10^{3}	3.6×10^{3}
200 W, Titanate	3.0×10^{5}	8.0×10^{4}	3.6×10^{4}	2.0×10^{4}	1.3×10^{4}	8.8×10^{3}	6.3×10^{3}	4.8×10^{3}	3.7×10^{3}	2.9×10^{3}
Ratio	1.23	1.13	1.11	1.15	1.23	1.14	1.21	1.21	1.24	1.24
500 W, Oxide	8.8×10^{5}	2.3×10^{5}	1.0×10^{5}	5.8×10^{4}	3.7×10^{4}	2.7×10^{4}	1.9×10^{4}	1.6×10^{4}	1.2×10^{4}	9.0×10^{3}
500 W, Titanate	7.0×10^{5}	1.7×10^{5}	7.8×10^{4}	4.3×10^{4}	2.7×10^{4}	1.9×10^{4}	1.4×10^{4}	1.1×10^{4}	8.5×10^{3}	6.8×10^{3}
Ratio	1.26	1.35	1.28	1.35	1.37	1.42	1.36	1.45	1.41	1.32
1000 W, Oxide	1.8×10^{6}	4.4×10^{5}	2.0×10^{5}	1.1×10^{5}	7.0×10^{4}	4.9×10^{4}	3.7×10^{4}	2.8×10^{4}	2.1×10^{4}	1.7×10^{4}
1000 W, Titanate	1.3×10^{6}	3.6×10^{5}	1.6×10^{5}	8.3×10^{4}	5.3×10^{4}	3.8×10^{4}	2.8×10^{4}	2.2×10^{4}	1.7×10^{4}	1.3×10^{4}
Ratio	1.38	1.22	1.25	1.33	1.32	1.29	1.32	1.27	1.24	1.31
2000 W, Oxide	3.7×10^{6}	8.8×10^{5}	3.9×10^{5}	2.2×10^{5}	1.5×10^{5}	9.8×10^{4}	7.2×10^{4}	5.6×10^{4}	4.3×10^{4}	3.4×10^{4}
2000 W, Titanate	2.7×10^{6}	7.0×10^{5}	2.9×10^{5}	1.6×10^{5}	1.0×10^{5}	7.3×10^{4}	5.4×10^{4}	4.0×10^{4}	3.2×10^{4}	2.5×10^{4}
Ratio	1.37	1.26	1.34	1.38	1.5	1.34	1.33	1.40	1.34	1.36
5000 W, Oxide	8.3×10^{6}	2.0×10^{6}	8.8×10^{5}	5.0×10^{5}	3.2×10^{5}	2.3×10^{5}	1.7×10^{5}	1.2×10^{5}	1.0×10^{5}	8.0×10^{4}
5000 W, Titanate	6.4×10^{6}	1.5×10^{6}	6.7×10^{5}	3.6×10^{5}	2.3×10^{5}	1.7×10^{5}	1.2×10^{5}	9.1×10^{4}	7.3×10^{4}	5.8×10^{4}
Ratio	1.30	1.33	1.31	1.39	1.39	1.35	1.42	1.32	1.37	1.38

TABLE 5 (Cont'd)

	Dose Rates (Rads/hr) and Dose Rate Ratios At									
	1 M	2 M	3 M	4 M	5 M	6 M	7 M	8 M	9 M	10 M
10,000 W, Oxide	1.5×10^{7}	3.8×10^{6}	1.7×10^{6}	9.1×10^{5}	6.0×10^{5}	4.2×10^{5}	3.1×10^{5}	2.3×10^{5}	1.8×10^{5}	1.5×10^{5}
10,000 W, Titanate	1.1×10^{7}	2.8×10^{6}	1.2×10^{6}	6.3×10^{5}	4.0×10^{5}	2.8×10^{5}	2.1×10^{5}	1.6×10^{5}	1.3×10^{5}	1.0×10^{5}
Ratio	1.36	1.36	1.42	1.44	1.50	1.50	1.48	1.44	1.38	1.50
20,000 W, Oxide	2.9×10^{7}	6.9×10^{6}	2.9×10^{6}	1.7×10^{6}	1.1×10^{6}	7.3×10^{5}	5.5×10^{5}	4.2×10^{5}	3.3×10^{5}	2.7×10^{5}
20,000 W, Titanate	2.1×10^{7}	4.9×10^{6}	2.1×10^{6}	1.2×10^{6}	7.1×10^{5}	5.0×10^{5}	3.8×10^{5}	2.9×10^{5}	2.3×10^{5}	1.9×10^{5}
Ratio	1.38	1.41	1.38	1.42	1.55	1.46	1.45	1.45	1.43	1.42

III.2 Fuel Release to the Atmosphere

Fuel release to the atmosphere by (1) evaporation from a melted capsule; (2) direct diffusion from a broached capsule; or (3) by resuspension from predeposited fuel on the ground may result in human exposure. Deposition of fuel particles on the skin, inhalation of these particles into the lungs or ingestion into the gastrointestinal tract will cause undesirable exposure. Particles deposited in the lung may be translocated to the GI tract or they may remain in the lung for a long period of time.

III.2.1 Doses to the Skin

Comparison in this case can be based on a per curie, per gram, or per cm^3 basis.* On a per curie basis doses delivered to the skin from ^{90}SrO particles would be slightly higher than those delivered by equally radioactive $^{90}SrTiO_3$ particles due to the attenuation of the β's in the larger titanate particles. This effect, however, is expected to be negligible.

On a per gram basis the dose ratio would be equal to the ratio of specific activities, i.e., 0.444 (W/g of oxide)/0.2525 (W/g of titanate) = 1.76 or 0.419/0.2335 = 1.79 for the average oxide and titanate (see Appendix B).

On a per cm^3 basis, i.e., ratio of doses delivered from equal size particles of oxide and titanate is 2.09 (W/cm^3 of oxide)/1.29 (W/cm^3 of titanate) = 1.62 or 1.94/1.17 = 1.66 for the average oxide and titanate fuel.

III.2.2 Doses to the GI Tract

Particles can be deposited in the GI tract either directly through ingestion of contaminated food or drink or indirectly through translocation of particles from the lung. The specific tissues at risk when $^{90}SrO/^{90}SrTiO_3$ particles reach the GI tract (according to recommendations of the International Commission on Radiological Protection (ICRP)[10]) are (1) for soluble ^{90}Sr, the bone while (2) that for insoluble ^{90}Sr is the lung and the lower large intestines (LLI). Hence, for oxide particles bone dose is decisive while for the titanate particles the LLI dose is more critical. Therefore, a direct hazard comparison between the two ^{90}Sr compounds is on this basis unfeasible. Comparison can be made by estimating the ratio of the amounts of ^{90}Sr reaching the bone from equal size particles (i.e., on a per cm^3 basis)

*The hazard may also depend upon the physical and chemical properties of the oxide or titanate which affect the distribution of the radioactivity over the skin surface.

of oxide and titanate deposited in the GI tract. Insomuch as the biological half-lives for particulates in the nasopharynx, and trachea to terminal bronchioles are of the order of 4 and 10 minutes respectively for particulates of all classes,[11] it is safe to assume that those particles end up in the GI tract. Hence, all the solubilization (if any) takes place during the particle residence time in the GI tract, i.e., no solubility takes place in the lungs unless the particles are deposited in the deep lung. Such particles will be treated below. It has also been established that a fixed fraction (9%) of the soluble ^{90}Sr absorbed in the GI tract reaches the bone[12] regardless of the chemical form of the soluble Sr-90 compound. In accord with the above discussion the relative bone doses would simply be the ratio of the amount of ^{90}Sr leached from the oxide particle to that from the titanate particle in the GI tract.

Strontium-90 oxide is quite soluble and should be expected to dissolve completely in the GI tract. The titanate fuel on the other hand has a very limited solubility which decreases with time to a minimum then increases again (see Appendix B) to a value around 1 mg/cm^2/day. Using this solubility rate, R, the amount of titanate leached off a microsphere of $^{90}SrTiO_3$ of mass M_o grams and radius r cm in time t days can be calculated as follows: The leaching rate is proportional to the surface area of the microsphere. Hence

$$\frac{dM}{dt} = - R(4\pi r^2) \qquad (1)$$

but $M = 4/3\ \pi r^3 \rho$ (where ρ is the density in g/cm^3)

$$\frac{dM}{dt} = - R\ \frac{(4\pi)^{1/3}\ (3M)^{2/3}}{\rho^{2/3}} \qquad (2)$$

Taking $\rho = 5.03$ g/cm^3, equation (2) becomes

$$\frac{dM}{dt} = - 1.6473\ R\ M^{2/3} \qquad (3)$$

The solution to this differential equation is

$$M = \left(M_o^{1/3} - 0.5491\ Rt\right)^3$$

$$= \left(M_o^{1/3} - 5.491 \times 10^{-4} t\right)^3 \qquad (4)$$

The amount leached is = $M_o - M$.

There is some disagreement on the transit time of particles through the GI tract. The standard-man data of the ICRP[13] are as follows:

Stomach (s)	1 hour
Small Intestine (SI)	4 hours
Upper Large Intestine (ULI)	8 hours
Lower Large Intestine (LLI)	18 hours
Total	31 hours

More recent work, however,[14,15] indicates that the values for ULI and LLI should be increased to 13 hours and 31 hours respectively. These data bring the total residence time to 49 hours.

Furthermore, studies conducted at the Argonne Cancer Research Hospital[15] using ^{134}Cs microspheres showed that the transit time varies widely among individuals. For the "average" subject, 36% of the dose remained in the GI tract on the third day after ingestion, 2.5% on the fifth day and < 0.1% up to the eleventh day. In view of these discrepancies solubility data were calculated for 1, 3 and 5 days of residence in the GI tract and relative hazards from the oxide/titanate particles of different sizes were calculated. It can be seen from Table 6 that the relative hazard to the bone varies from 1.6 to 72 depending on the particle size and the GI transit time.

The hazard to the GI tract itself should also be considered. Strontium-90 oxide particles would most probably dissolve completely in the stomach and mix with its contents. Therefore, the radiation dose to the stomach walls would be diffused and it can be considered negligible. At lower points in the tract, where contents become fluid and where walls of the intestine are no longer distended, relatively higher doses may be encountered. On the other hand, intact titanate particles would cause more intense local irradiation of the GI tract walls.

It is difficult to estimate the average dose delivered by a titanate particle moving within a food bolus. Assuming that the particle settles on the epithelial lining, it is possible to calculate the "hot particle" dose to the sensitive layer of the GI tract located 300μ under the surface. This naturally represents the worst possible case. Table 7 shows calculated dose rates to an area of 1 cm^2 for different size particles. It is seen from the table that if such a situation is realized even the smallest particles can deliver, in a matter of hours, doses exceeding the maximum allowable yearly dose of 15 rems to a limited area of the GI tract.[10] Within these few hours the particle size can be considered practically constant.

TABLE 6

COMPARISON BETWEEN DISSOLVED AMOUNTS OF $^{90}SrTiO_3$ AND ^{90}SrO IN THE GI TRACT

Particle Diameter, μ	Time, Days	Original Mass of Titanate, g	Mass of Titanate Remaining, g	Dissolved Titanate Activity, Ci	Dissolved Oxide Activity, Ci	Ratio of Oxide to Titanate
5	1.00	0.3292e-09*	0.2857e-11	0.1136e-07	0.1893e-07	0.1667e 01**
10	1.00	0.2634e-08	0.5776e-09	0.7155e-07	0.1514e-06	0.2116e 01
20	1.00	0.2107e-07	0.1086e-07	0.3553e-06	0.1212e-05	0.3410e 01
50	1.00	0.3292e-06	0.2572e-06	0.2507e-05	0.1893e-04	0.7550e 01
100	1.00	0.2634e-05	0.2335e-05	0.1040e-04	0.1514e-03	0.1457e 02
200	1.00	0.2107e-04	0.1986e-04	0.4211e-04	0.1212e-02	0.2877e 02
500	1.00	0.3292e-03	0.3217e-03	0.2621e-03	0.1893e-01	0.7222e 02
5	3.00	0.3292e-09	0.000	0.1146e-07	0.1893e-07	0.1652e 01
10	3.00	0.2634e-08	0.000	0.9166e-07	0.1514e-06	0.1652e 01
20	3.00	0.2107e-07	0.1391e-08	0.6848e-06	0.1212e-05	0.1769e 01
50	3.00	0.3292e-06	0.1456e-06	0.6389e-05	0.1893e-04	0.2963e 01
100	3.00	0.2634e-05	0.1802e-05	0.2895e-04	0.1514e-03	0.5231e 01
200	3.00	0.2107e-04	0.1754e-04	0.1228e-03	0.1212e-02	0.9864e 01
500	3.00	0.3292e-03	0.3065e-03	0.7918e-03	0.1893e-01	0.2391e 02
20	5.00	0.2107e-07	0.5926e-14	0.7332e-06	0.1212e-05	0.1652e 01
50	5.00	0.3292e-06	0.7214e-07	0.8946e-05	0.1893e-04	0.2116e 01
100	5.00	0.2634e-05	0.1357e-05	0.4444e-04	0.1514e-03	0.3408e 01
200	5.00	0.2107e-04	0.1541e-04	0.1970e-03	0.1212e-02	0.6150e 01
500	5.00	0.3292e-03	0.2917e-03	0.1305e-02	0.1893e-01	0.1451e 02

*e-07 ≡ 10^{-7}
**e 01 = 10^{1}

TABLE 7

DOSE RATES DELIVERED BY $^{90}SrTiO_3$ PARTICLES AVERAGED OVER 1 CM^2 AREA AT 300μ DEPTH IN TISSUE

Particle Diameter, μ	β-Dose Rate, rems/hr
10	1.14×10^{-1}
20	9.48×10^{-1}
50	9.48
100	8.06×10^{1}
150	2.37×10^{2}
200	5.21×10^{2}
250	9.48×10^{2}
300	1.52×10^{3}

It is worth mentioning here that a particle of ^{90}SrO has to be about 60μ in diameter to be able to deliver, when completely dissolved in the GI tract, 2 microcuries* of ^{90}Sr to the bone. It seems, therefore, that the maximum allowable yearly dose to the GI tract can be exceeded from a titanate particle of a smaller size than that of a ^{90}SrO particle necessary to supply the maximum permissible bone burden of ^{90}Sr.

Two points should be emphasized here. The comparsion is made between doses delivered to two different organs in the above paragraph. The assumption being that maximum allowable doses to different organs of the body represent equal levels of risk to the human body. In addition, the actual dose delivered to the GI tract may be less by orders of magnitude than those estimated in Table 7 if the titanate particle remains suspended in the bolus.

III.2.3 Doses to the Lungs

Strontium-90 oxide particles deposited in the pulmonary or lymph regions of the lung are expected to dissolve in a short time distributing ^{90}Sr to the blood, bone and other organs. Titanate particles deposited in the same region are not expected to have more than an aerodynamic diameter (actual diameter x $(\text{density})^{1/2}$) of 10μ. For average $^{90}SrTiO_3$ fuel this is equivalent to an actual diameter of $\frac{10}{\sqrt{5.03}}$ or about 4μ.[11] A titanate particle of this size dissolves completely in a little over a day as can be seen from Table 6. Comparing such an interval of time to an assumed lung residence time of weeks for class W type particles to which $^{90}SrTiO_3$ can be assigned,[11] it can be assumed that the particle would dissolve completely distributing roughly 56% as much ^{90}Sr to the different body organs as would a ^{90}SrO particle of equal size. On the other hand, it would have delivered (as an intact particle) about 0.2 rads of β dose to the lung before complete dissolution.

III.3 Fuel Release in the Ocean

Post implantation, the principal radiation hazard from a marine radioisotopic unit is from the release of fuel by solubility in seawater through a breach in the capsule. Two areas are of great concern in such a situation; transport of the dissolved fuel in the ocean environment and the biological implications of this dissolution and transport. The first area will be treated here in detail but the last will be only summarized, from reference 2, in Section IV.

*Maximum permissible bone burden of ^{90}Sr as recommended in reference 12

In the absence of experimental data for a direct comparison of potential hazards resulting from equivalent marine sources of ^{90}SrO and $^{90}SrTiO_3$, an ocean diffusion model is used to describe the temporal and spatial distribution of the radioactivity. Such a model must be capable of: (1) differentiating between an instantaneously soluble source of activity, the ^{90}SrO, and a continuous, slowly soluble source, $^{90}SrTiO_3$, (2) calculating volumes of water contaminated to different activity levels, time durations over which such contamination lasts and amounts of activity enclosed within isoconcentration contours. With such information at hand the second area of concern, i.e., the biological implications can be estimated.

Several ocean diffusion models, most of which are two-dimensional, have been developed. Smith[16] summarized these models and compared their characteristics. A more recent, comprehensive survey of existing two and three dimensional diffusion models revealed that the Carter-Okubo[3] model was the only three-dimensional ocean model for which data were available for evaluating its required empirical constants. Although a number of experiments have been conducted in lakes, rivers, and bays the data obtained from these experiments were in general not applicable to a three-dimensional model. This model is considered much more realistic than the two-dimensional models which assume a completely uniform distribution of radioactivity along the third dimension (vertical) regardless of the water depth.

III.3.1 General Description of the Carter-Okubo Model

The basic differential equation in the Carter-Okubo model may be written as:[3]

$$\frac{\partial s}{\partial t} + (V_o - \Omega_y Y - \Omega_z Z)\frac{\partial s}{\partial x} = A_x\frac{\partial^2 s}{\partial x^2} + A_y\frac{\partial^2 s}{\partial y^2} + A_z\frac{\partial^2 s}{\partial z^2} \qquad (5)$$

where $s(t,x,y,z)$ is the concentration in Ci/m^3. This differential equation represents an ocean turbulence system which consists of both large and small scale eddies. The large scale eddies are represented by the Ω_z and Ω_y terms, and the small scale eddies by the A_x, A_y and A_z terms.

The large scale eddies are grossly represented by a nonuniform velocity field chosen for convenience as linear in y and z but independent of x. The Omega terms may hence be regarded as constant horizontal (Ω_y) and vertical (Ω_z) shears (velocity gradients) which introduce

inhomogeneity into the differential equation. The horizontal shear Ω_y determined from dye tests is, in general, much larger than the vertical shear Ω_z.

The mean velocity may be expressed by equation (6) if the coordinate system is taken such that the mean current flow is in the x direction.

$$\bar{V}_x = V_o - \Omega_y Y - \Omega_z Z \text{ and } \bar{V}_y = \bar{V}_z = 0 \qquad (6)$$

The small-scale eddies arise as a result of internal mixing. Since this effect is small, and is associated with times which are small in comparison to the time of interest, the mixing length theory for dye diffusion may be utilized. This theory assumes that the eddy diffusivity is constant with respect to time and space but is anisotropic at each point as characterized by unique and different values of A_x, A_y and A_z.

III.3.2. Instantaneous Point Source Release

Reference 3 obtains a solution for the partial differential equation, based on an instantaneous point source release in an infinite ocean medium. This solution eliminates the constant current term, V_o from equation (4) by the method indicated above, i.e., by taking a coordinate system moving with velocity V_o in the x direction. As an initial condition the total amount of radioactivity M (in curies) is assumed to be instantaneously released from the origin at time t = 0. By then assuming a small perturbation $\delta(x).\delta(y).\delta(z)$ where the operator δ represents the dirac delta function, Fourier transforming, and integrating over infinite space, a solution is obtained:(3)

$$s(t,x,y,z) = \qquad (7)$$

$$\frac{M \exp\left\{-\frac{1}{4t(1+Bt^2)}\left[\frac{x'^2}{A_x}+\frac{(1+B_y t^2)y^2}{A_y}+\frac{(1+B_z t^2)z^2}{A_z}+\frac{(\Omega_y y+\Omega_z z)tx'+\frac{1}{2}\Omega_y\Omega_z yzt^2}{A_x}\right]\right\}}{8\pi^{3/2}\sqrt{A_x A_y A_z}\, t^{3/2}\sqrt{1+Bt^2}}$$

where $B = \frac{1}{12}\left(\frac{\Omega_y^2 A_y}{A_x}+\frac{\Omega_z^2 A_z}{A_x}\right)$

$$B_y = \frac{1}{3}\frac{\Omega_y^2 A_y}{A_x} + \frac{1}{12}\frac{\Omega_z^2 A_z}{A_x}$$

$$B_z = \frac{1}{12}\frac{\Omega_y^2 A_y}{A_x} + \frac{1}{3}\frac{\Omega_z^2 A_z}{A_x}$$

It may be observed from equation (7) that for given values of s and t the solution is quadratic in x,y,z and as such represents a family of ellipsoids. The ellipsoids are regular in shape but the orientation of their principal axes varies with time. Equation (7) also states that the dimensions of the principal axes will be functions of $A_x, A_y, A_z, \Omega_y, \Omega_z$ and time.

In applying such an instantaneous release model, the assumption is made that the fuel is infinitely soluble in sea water, i.e., once a fuel capsule is broken open the fuel is assumed to be completely dissolved. This assumption will, of course, never be fully realized. However, this approach to the solution of the instantaneous problem does represent the most hazardous possible condition resulting from instantaneous release.

III.3.2.1 NRDL Instantaneous Digital Computer Code*

The basic solution (equation (7)) yields only the concentration as a function of both time and space coordinates. In order to evaluate the biological effects of an instantaneous release of radioactivity in the ocean, however, the volume of ocean water contaminated, the dimensions of that volume, and the total amount of radioactivity present in the volume are needed. Further discussion on this point will be included in Section IV.

III.3.2.1a Calculation of the Contaminated Volume

The volume of ocean water containing concentrations equal to or greater than a given concentration (i.e., 1 MPCC or multiples thereof) may be calculated from the basic Okubo-Carter result (equation (7)) as follows: Equation (7) may be rewritten in the form of a general quadratic equation:

*This Code and the Continuous Code discussed later are under development by NRDL for Sandia Corporation under Purchase Order No. ASB 48-6183.

$$\frac{x'^2}{A_x} + \frac{(1+B_y t^2)y^2}{A_y} + \frac{(1+B_z t^2)z^2}{A_z} + \frac{t\Omega_y x'y}{A_x} + \frac{t\Omega_z x'z}{A_x} + \frac{1/2\ \Omega_y\Omega_z t^2 yz}{A_x} + C_{s,t} = 0$$

where:

$$C_{s,t} = -4t(1+Bt^2)\ \ln\left(\frac{M_o}{s\ 8\pi^{3/2}\sqrt{A_x A_y A_z}\ t^{3/2}\sqrt{1+Bt^2}}\right) \qquad (8)$$

It is possible to transform any proper quadratic equation to one of the standard conical forms. The standard conical form for an ellipsoid is,

$$\frac{x^2}{a^2} + \frac{y^2}{b^2} + \frac{z^2}{c^2} = 1 \qquad (9)$$

where a, b, and c are the semi axes of the ellipsoid.

The volume of the ellipsoid is then expressed by:

$$V = \frac{4}{3}\pi\ abc \qquad (10)$$

The volume as a function of time may be obtained from equation (10) by utilizing the relationships expressed in equations (12), (13) and (14) where the coefficients in the determinants A and B are defined by the following generalized quadratic equation and by equation (8).

$$(a_{11}x + a_{12}y + a_{13}z + a_{14})x + (a_{21}x + a_{22}y + a_{23}z + a_{24})y + (a_{31}x + a_{32}y + a_{33}z + a_{34})z + (a_{41}x + a_{42}y + a_{43}z + a_{44}) = 0 \qquad (11)$$

$$a^2 = -\frac{1}{\lambda_3}\frac{A}{D} \qquad (12a)$$

$$b^2 = -\frac{1}{\lambda_2}\frac{A}{D} \qquad (12b)$$

$$c^2 = -\frac{1}{\lambda_1}\frac{A}{D} \qquad (12c)$$

$$A = \begin{vmatrix} a_{11} & a_{12} & a_{13} & a_{14} \\ a_{21} & a_{22} & a_{23} & a_{24} \\ a_{31} & a_{32} & a_{33} & a_{34} \\ a_{41} & a_{42} & a_{43} & a_{44} \end{vmatrix} \quad \text{and } D = \begin{vmatrix} a_{11} & a_{12} & a_{13} \\ a_{21} & a_{22} & a_{23} \\ a_{31} & a_{32} & a_{33} \end{vmatrix} = \lambda_1\lambda_2\lambda_3$$

The determinant A may be expressed in terms of D by noting a_{41}, a_{42}, a_{43}, a_{14}, a_{24}, and $a_{34} = 0$.

$$A = \begin{vmatrix} a_{11} & a_{12} & a_{13} & 0 \\ a_{21} & a_{22} & a_{23} & 0 \\ a_{31} & a_{32} & a_{33} & 0 \\ 0 & 0 & 0 & C_{s,t} \end{vmatrix} = C_{s,t}\, D$$

$$\text{Hence } V = \frac{4}{3}\pi\sqrt{\frac{-A^3}{\lambda_1\lambda_2\lambda_3 D^3}} = \frac{4\pi}{3}\sqrt{\frac{-C_{s,t}^3}{\lambda_1\lambda_2\lambda_3}} = \frac{4}{3}\pi\frac{(-C_{s,t})^{3/2}}{D^{1/2}} \qquad (13)$$

From the definition of $C_{s,t}$ the expression for the volume may be written as equation (14).

$$V(t) = \frac{4}{3}\pi\frac{\left[4\tau(1+B\tau^2)\ln\left(\dfrac{M_o}{s\sigma\pi^{3/2}\sqrt{A_x A_y A_z}\, t^{3/2}\sqrt{1+Bt^2}}\right)\right]^{3/2}}{D^{1/2}} \qquad (14)$$

The effect of the mean velocity term v_o (i.e., current) on the volume of contaminated water, can be checked by performing the following steps:

(1) Assume a fixed coordinate system x related to the moving coordinate system x' by:

$$x' = x - v_o t \qquad (15)$$

(2) Substitute this expression for x' in equation (8).

(3) Evaluate the determinants A and B in terms of the new coefficients $a_{ij}(k)$.

(4) Cancel all like terms and solve for the volume.

The result of this exercise leads identically to equation (14). It may thus be stated that the volume of the patch is independent of the mean current velocity v_o in the instantaneous point source release case.

The volume containing concentrations equal to or greater than a given concentration D_o (expressed as multiples of MPCC), may be calculated from equation (14) by choosing $s = D_o$. A volume vs time curve may then be obtained from equation (14) by calculating the volume at various times, from t = 0 to t = T (where T represents some specified time of interest).

III.3.2.1b Time-Averaged Volume Calculation

A time-averaged volume representing concentrations greater than a specified concentration (1 MPCC for example) may be calculated by integrating equation (14) over the time of interest, T, as follows:

$$\bar{V} = \frac{1}{T}\int_o^T V dt = \frac{32\pi}{3T}\int_o^T \left[\frac{t\left(1+Bt^2\right)\ln\left(\frac{M_o}{s\delta\pi\sqrt{A_x A_y A_z}\, t^{3/2}\sqrt{1+Bt^2}}\right)}{D^{1/2}(t)}\right]^{3/2} dt \qquad (16)$$

This integration is performed numerically in the NRDL instantaneous digital computer program by dividing the time interval T into N equal parts ($T = N\Delta t$), calculating the volume V_i at each Δt increment, summing and averaging:

$$\bar{V} = \frac{1}{N\Delta t}\sum_{i=1}^{N} V_i\,\Delta t = \frac{1}{N}\sum_{i=1}^{N} V_i \qquad (17)$$

III.3.2.1c Calculation of the Ellipsoid Dimensions

The principal axes of the contaminated ellipsoidal volume may be found by solving the characteristic equation defined by the following determinant:(17)

$$\begin{vmatrix} a_{11}-\lambda & a_{12} & a_{13} \\ a_{21} & a_{22}-\lambda & a_{23} \\ a_{31} & a_{32} & a_{33}-\lambda \end{vmatrix} = 0 \qquad (18)$$

The resulting equation (18) may be obtained by defining the coefficients a_{ij} from equations (8) and (11) and expanding the determinant.

$$\lambda^3 + \left(\frac{1}{A_x} + \frac{1+B_y t^2}{A_y} + \frac{1+B_z t^2}{A_z}\right)\lambda^2 \qquad (19)$$

$$- \left[\left(\frac{t\Omega_y}{2A_x}\right)^2 + \left(\frac{t\Omega_z}{2A_x}\right)^2 + \left(\frac{t^2\Omega_y\Omega_z}{4A_x}\right)^2 - \left(\frac{1}{A_x}\right)\left(\frac{1+B_y t^2}{A_y}\right) - \left(\frac{1}{A_x}\right)\left(\frac{1+B_z t^2}{A_z}\right) - \left(\frac{1+B_y t^2}{A_y}\right)\left(\frac{1+B_z t^2}{A_z}\right)\right]\lambda$$

$$- \left[\left(\frac{1}{A_x}\right)\left(\frac{1+B_y t^2}{A_y}\right)\left(\frac{1+B_z t^2}{A_z}\right) + 2\left(\frac{t\Omega_y}{2A_x}\right)\left(\frac{\Omega_y\Omega_z t^2}{4A_x}\right)\left(\frac{t\Omega_z}{2A_x}\right) - \left(\frac{1}{A_x}\right)\left(\frac{\Omega_y\Omega_z t^2}{4A_x}\right)^2 - \left(\frac{t\Omega_y}{2A_x}\right)^2\left(\frac{1+B_z t^2}{A_z}\right) -$$

$$- \left(\frac{t\Omega_z}{2A_x}\right)^2\left(\frac{1+B_y t^2}{A_y}\right)\right] = 0$$

The characteristic eigenvalues of the matrix $(\lambda_1, \lambda_2, \lambda_3)$ may be found by solving this cubic equation.

The semi-axes a, b, and c are then calculated from the relationships defined in equations (12a), (12b), and (12c).

III.3.3 Continuous Point Source Ocean Release

The continuous ocean diffusion model assumes that radioactive fuel in a slowly dissolving form has been deposited in the ocean and is continuously releasing radioactivity. This situation exists in the case of $SrTiO_3$ fuel. A mathematical model and a digital computer code which calculates the distribution of the radioactivity based upon both diffusion, and ocean current convection are being developed at NRDL.[4]

The digital model presently consists of numerically integrating the basic Carter-Okubo differential equation until essentially steady state conditions are reached at a given time and distance from the fixed source.

Once the steady state concentration distribution is determined the computer code calculates the parameters of volume, dimensions, and fractional amount of radioactivity present within a given concentration isopleth.

III.3.3.1 NRDL Continuous Digital Computer Code

The Carter-Okubo solution to the instantaneous point source problem has been employed as the kernel in a time integration to obtain the concentration field in an infinite ocean environment resulting from a point continuous source. It may be recalled that the instantaneous source result was presented in a spatial coordinate system that moves in the x-direction at the mean current velocity v_o. We may construct the solution for the continuous source case for either of two source conditions.

a. The source may be assumed to move with the water at the velocity v_o.

b. The source may be assumed to remain in a fixed geographic position and the water moves past it at the velocity v_o.

Case (a) would correspond approximately to the practical problem of a source mounted on a freely moving buoy whereas case (b) might be related to a nuclear source lying on the ocean floor or to an anchored buoy situation. In any of the real situations the proximity of a boundary, e.g., surface or ocean floor, invalidates the Carter-Okubo point instantaneous kernel. However, the mathematics for semi-infinite environments have yet to be developed and we may expect to obtain some useful approximation from the infinite ocean assumption. The present NRDL Continuous Source Code solves the infinite ocean problem for the fixed source (Case (b) above). It considers a continuous radioactivity source dissolving at the rate of R(t) per unit time as a series of instantaneous releases.

Now we consider the concentration field, in the fixed coordinate system with origin at the source location, that results from an instantaneous source of $R = R(t)dt$. To use the Carter-Okubo result in this coordinate system we must transform it back to the fixed reference. We consider the solution in the form of equation (7) as $S_I(R,x',y',z',\tau)$ where x', y', z' are the spatial coordinates in the moving reference and

τ is the time measured from the time of release. The fixed coordinate system is related by the transformation

$$x = v_o\tau + x'$$

$$y = y'$$

$$z = z'$$

Consequently the desired point instantaneous kernel is given by the form of equation (7) expressed as

$$S_I(R,x-v_o\tau,y,z,\tau) = \frac{R}{8\pi^{3/2}\sqrt{A_xA_yA_z}\,\tau^{3/2}\sqrt{1+B\tau^2}} \exp\left\{-\frac{1}{4\tau(1+B\tau^2)}\right.$$

$$\left.\left[\frac{(x-v_o\tau)^2}{A_x} + \frac{(1+B_y\tau^2)y^2}{A_y} + \frac{(1+B_z\tau^2)z^2}{A_z} + \frac{(\Omega_y y+\Omega_z z)(x-v_o\tau)\tau}{A_x} + \frac{\Omega_y\Omega_z\tau^2 yz}{2A_x}\right]\right\}$$

This may be written more compactly in the form

$$S_I(R,x-v_o\tau,y,z,\tau) = \frac{R\exp\left[-\frac{(\alpha+B\tau+\gamma\tau^2)}{4(1+B\tau^2)\tau}\right]}{8\pi^{3/2}\sqrt{A_xA_yA_z}\,\tau^{3/2}\sqrt{1+B\tau^2}} \tag{20}$$

where

$$\alpha = \frac{x^2}{A_x} + \frac{y^2}{A_y} + \frac{z^2}{A_z} \tag{21a}$$

$$\beta = -\frac{2v_o x}{A_x} + \frac{\Omega_y xy}{A_x} + \frac{\Omega_z xz}{A_x} \tag{21b}$$

$$\gamma = \frac{v_o^2}{A_x} + \frac{B_y y^2}{A_y} + \frac{B_z z^2}{A_z} - \frac{v_o(\Omega_y y+\Omega_z z)}{A_x} + \frac{\Omega_y\Omega_z yz}{2A_x} \tag{21c}$$

To obtain the concentration field resulting from a continuous sequence of instantaneous sources R, we employ a Duhamel type integral[18]

$$S(x,y,z,T) = \int_o^T R(T-\tau)S_I(x-v_o\tau,y,z,\tau)\,d\tau \tag{22}$$

The independent time variable T is measured from the time of placement of the continuous source.

It is important to correctly interpret this result in terms of the source properties. In the most general sense we have a transient concentration field. However, the time dependence of the source strength will remain almost constant during the period of time T_o required for the concentration to reach a steady state in the field of interest. This quasi steady state condition applies for the case of interest and forms the basis of the present NRDL code. We are then concerned only with the steady state concentration and not the initial transient.

The source time dependence can be estimated from the consideration of the dissolution of a cylindrical element of radioactive material.(19)

$$M(t) = (M_o^{1/3} - CT)^3 \tag{23}$$

where C is a constant dependent upon the solubility of the material. The source strength is then

$$R(T) = -A\frac{dM}{dt} = 3CA\,(M_o^{1/3}-CT)^2 \tag{24}$$

where A is the activity per unit mass of the dissolving material. Equation (24) may be simplified to read

$$R(T) = (a + bT)^2 \tag{25}$$

where

$$a = \sqrt{3CA}\, M_o^{1/3}$$

$$b = -C\sqrt{3CA}$$

For each position in space (x,y,z) the integration of (17) is accomplished numerically to a time T_o beyond which no further increase in S results.

The continuous code must perform a large number of numerical integrations of the instantaneous Carter-Okubo solution (Equation 16) over time in order to obtain a continuous quasi-steady state solution. The code presently calculates steady state concentration at points in a 20 x 20 grid in the yz plane, and searches this grid to determine the coordinates of specified isoconcentration contours. By then calculating the areas bounded by the isoconcentration contours, incrementing in the x direction, calculating additional 20 x 20 yz grids for each new x increment, and integrating over x, the volumes enclosed by selected isoconcentration surfaces are obtained. Hence, if x is divided into 20 increments equation (16) must be evaluated numerically 8000 times (20 x 20 x 20) in order to describe the steady state concentration field over the desired range of concentration.

The Numerical integration over time consists of taking both constant and variable time steps.. The following figure illustrates this technique.

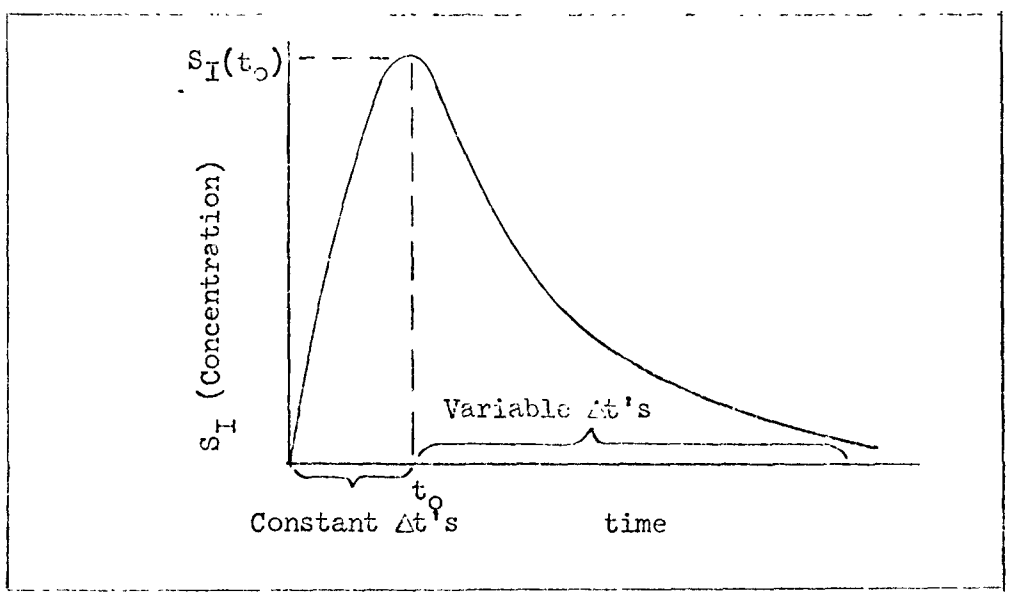

This typical curve represents the contribution at a particular spatial point from an instantaneous point source release at the origin of the coordinate system at time $0 \leq t \leq T$. Integrating to an appropriately large T yields the steady state solution.

The constant time step increments are determined by estimating a time (t_o) near the peak of the instantaneous concentration vs time curve. This time is estimated using the following equations:

$$t_o = \frac{x}{v_o} \text{ for } x > \frac{A_x}{v_o} \tag{26a}$$

$$t_o = \frac{x}{v_o} + \frac{y^2}{6A_y} + \frac{z^2}{6A_z} \text{ for } 0 < x < \frac{A_x}{v_o} \tag{26b}$$

$$t_o = \frac{x^2}{6A_x} + \frac{x}{v_o} \text{ for } x < 0 \tag{26c}$$

Equation (21a) is used for relatively large values of x where convection is the dominate mechanism for transport of the radioactive material. Equation (21b) is used for calculating concentrations near the source. The first term in this equation is the amount of time required for convection while the last two terms represent the time needed for diffusion in the y and z directions respectively. For diffusion in the negative x direction (i.e., against the mean current direction) the convection term must be substracted from the diffusion term (equation 21c). Each criterion for t_o has been chosen to ensure that it will be larger than the time at which the actual peak occurs.

The constant time step is then determined by

$$\Delta t_c = \frac{t_o}{N} \text{ for } t < t_o \tag{27}$$

where N is the number of desired increments (usually 100).

The use of a variable time step for $t > t_o$ reduces the number of required calculations by utilizing a time relaxation technique. The length of the time step is determined by

$$\Delta t_i = \Delta t_{i-1} \frac{S_I(t_o)}{S_I(t)} \text{ for } t > t_o \tag{28}$$

where $S_I(t_o)$ is the instantaneous concentration at t_o and $S_I(t)$ is the concentration at time t.

Since $S_I(t)$ is always decreasing as time increases beyond t_o and $S(t_o)$ is the maximum instantaneous concentration, the time step will become larger as time increases.

The integration is terminated when quasi-steady state conditions are reached. Such condition is considered to be achieved when the integrated concentration changes by less than a predetermined increment.

The continuous code may also be used to evaluate the inventory of activity within isoconcentration contours and compare it to the total activity released by the source in the time T_o required to reach steady state.

III.3.4 Results

This section of the report presents the results obtained from both instantaneous and continuous releases. The instantaneous cases considered are the release of 7.46×10^4 and 1.492×10^5 Ci of ^{90}SrO from 500 and 1000 watt capsules respectively. A sample of the computer plotted output and values obtained from a parametric study are included. The results of a continuous release of 7.46×10^4 Ci of $^{90}SrTiO_3$ are also presented.

III.3.4.1 Instantaneous Release

Results obtained from the instantaneous code indicate the existence of a relatively large volume of contaminated water containing concentrations greater than one MPCC early in the diffusion process. Figures 2 through 5 present examples of computer plotted outputs from the instantaneous diffusion code. The problem solved simulates the instantaneous release of approximately 75,000 Ci of Sr^{90} oxide from a 500 watt capsule.

Figure 2 shows the volume of sea water containing concentrations equal to or greater than 3.4×10^{-5} Ci/m^3 (i.e., 1 MPCC of Sr^{90}) as a function of time. The values used for the eddy diffusivities (A_x, A_y, A_z) and the horizontal and vertical shears (Ω_y and Ω_z) were obtained from empirical data representing August conditions in the coastal waters of the Cape Kennedy area. Table 8 summarizes those data.

Figure 3 presents a plot of the percent of radioactivity contained within the 1 MPCC isopleth as a function of time. It may be noted from this figure that there are no concentrations greater than 1 MPCC after approximately 175 hours.

TABLE 8

EMPIRICAL, DIFFUSION CONSTANTS

(CAPE KENNEDY, AUGUST CONDITIONS)[3]

$$A_x = 1400.\,m^2/hr$$

$$A_y = 1400.\,m^2/hr$$

$$A_z = 0.47\ m^2/hr$$

$$\Omega_y \ll \Omega_z \frac{A_z}{A_x} \simeq 0$$

$$\Omega_z = 23.8\ hr^{-1}$$

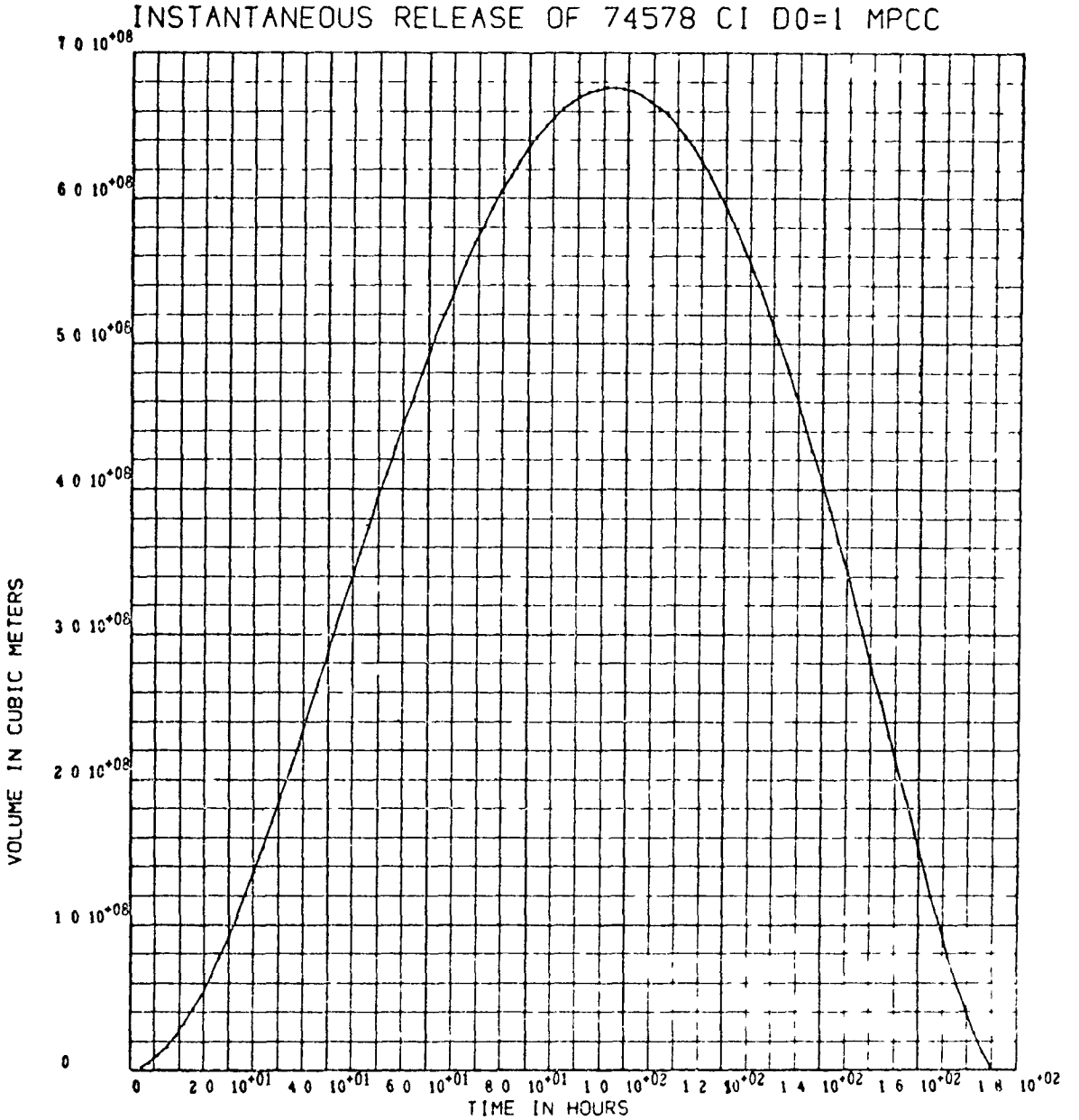

Figure 2. Computer Plotted Output for Volume vs. Time

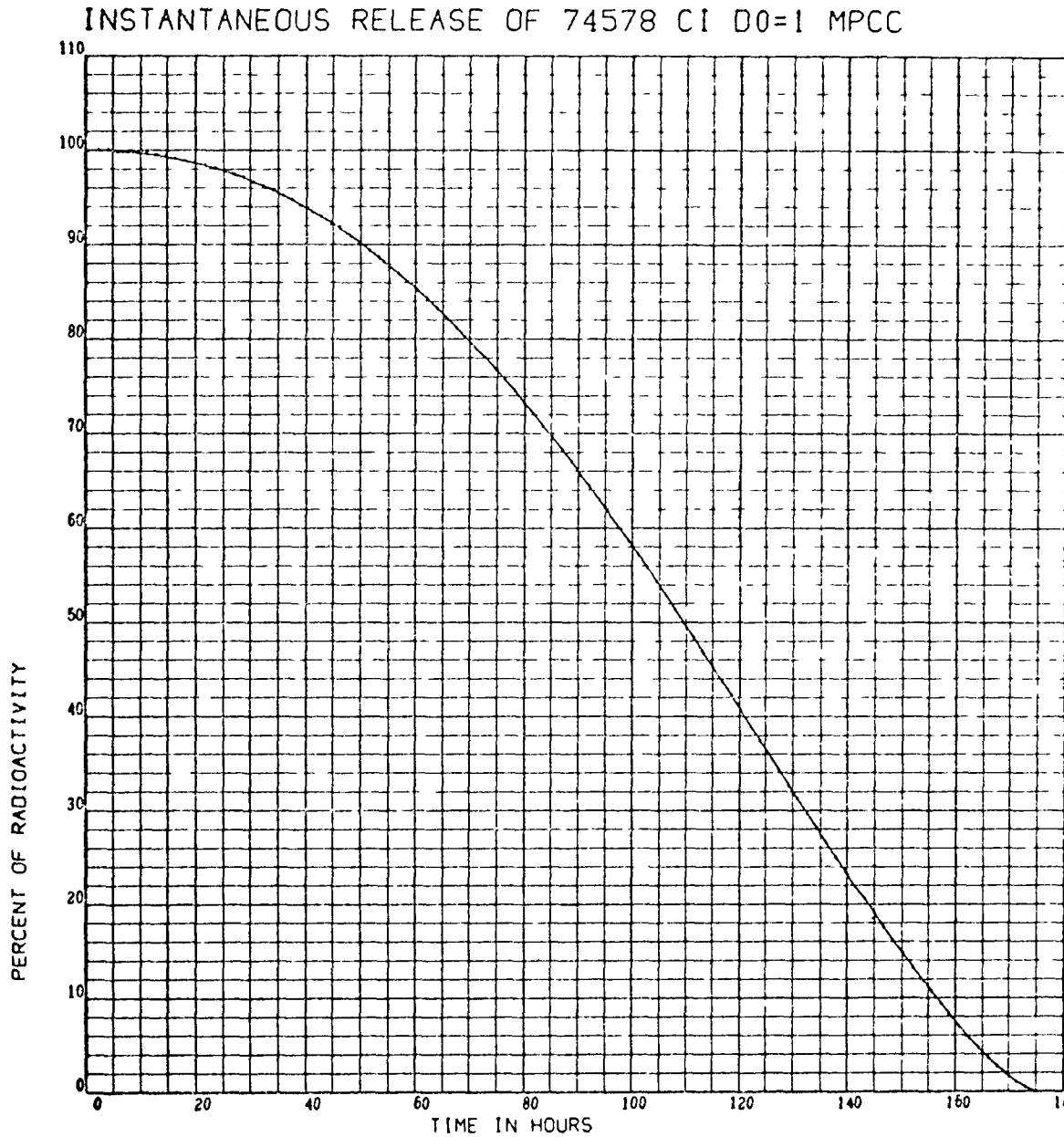

Figure 3. Computer Plotted Output for Percent Radioactivity vs. Time

Figures 4a through 4c show the dimensions of the semi-axes of the ellipsoid as a function of time. It may be observed from Figure 4c that the C axis of the ellipsoid, which approximately corresponds to the vertical dimension z, is much smaller than either the A or B axes which approximately represent the y and x dimensions respectively (Figures 4a and 4b).

III.3.4.2 Instantaneous Release Parametric Study

The results of a parametric study for instantaneous point source releases of 7.4×10^4 Ci, and 1.492×10^5 of Sr^{90} oxide have been obtained. The objective of this study was to determine the effect of empirical constants ($\Omega_y, \Omega_z, A_x, A_y, A_z$) on the instantaneous model. Each of the empirical constants was changed while holding all the other constants. The results obtained were compared to a standard instantaneous diffusion solution in which the values of the empirical constants represented August conditions at Cape Kennedy.

The values obtained from the parametric study are summarized in Table 9. Column one of this table indicates the only parameter which was varied from its standard value. The values of each variable recorded in Table 9 were those corresponding to the time t_{max} at which the volume within the 1 MPCC surface was a maximum. The other quantities recorded in Table 9 are defined as follows:

Multiplication Factor = The factor by which the standard empirical constant was multiplied in order to obtain the new value specified in column one.

T = The time beyond which no concentration greater than 1 MPCC exists (1 MPCC = 3.4×10^{-5} Ci/m3).

a, b, and c = The principal semi-axes of the ellipsoidal contaminated volume at t_{max}.

It may be observed from Table 9 that the maximum volume of contaminated water contained within a 1 MPCC isoconcentration surface is constant for a given source. This result implies that the maximum volume is a constant which depends only on the amount of radioactivity released, and the specified isoconcentration surface. The following analysis was performed in order to verify that the maximum volume is independent of the empirical constants in the Carter-Okubo instantaneous model.

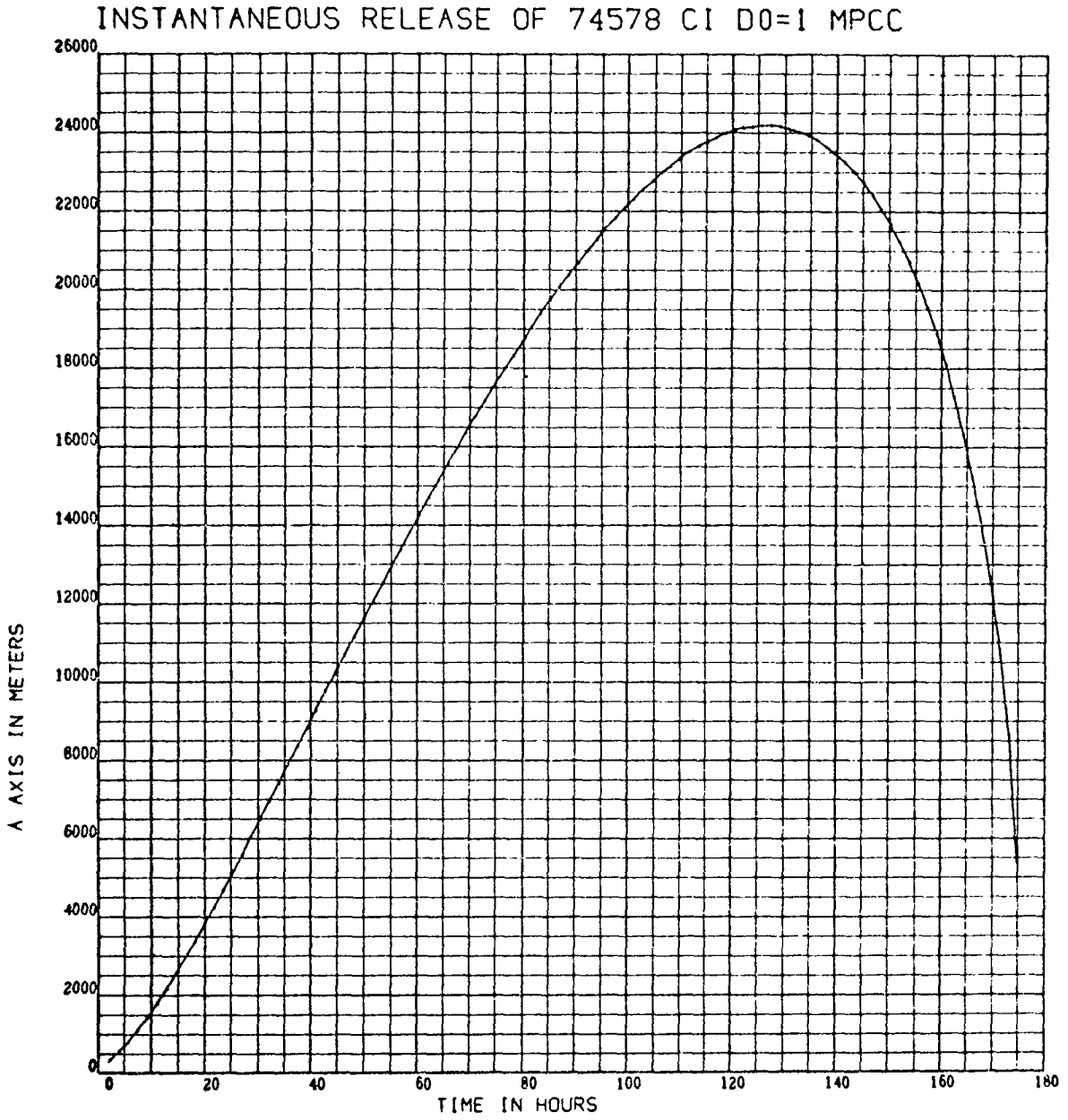

Figure 4(a). Computer Plotted Output for Ellipsoid Semi-Axis (A) vs. Time

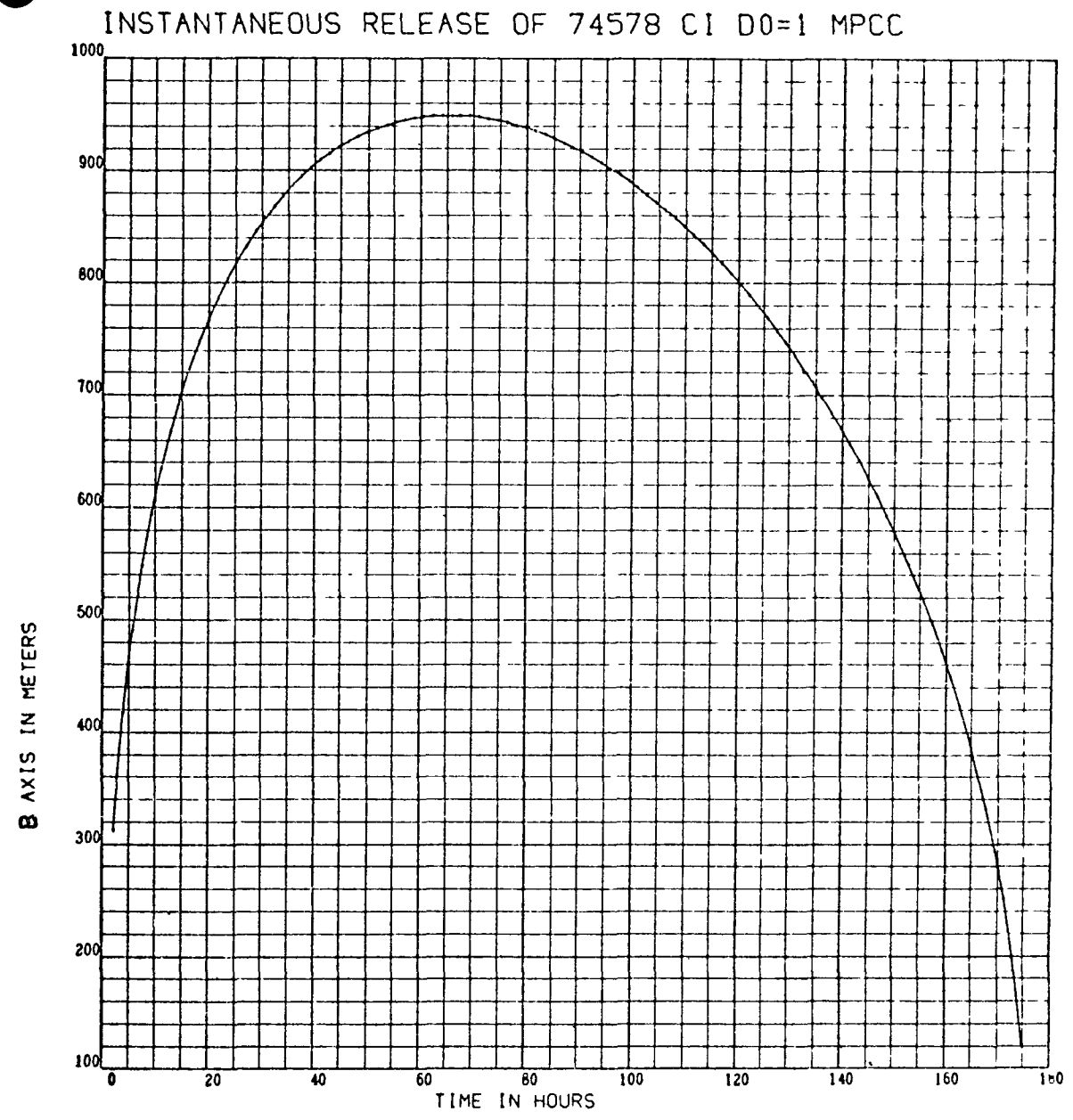

Figure 4(b). Computer Plotted Output for Ellipsoid Semi-Axis (B) vs. Time

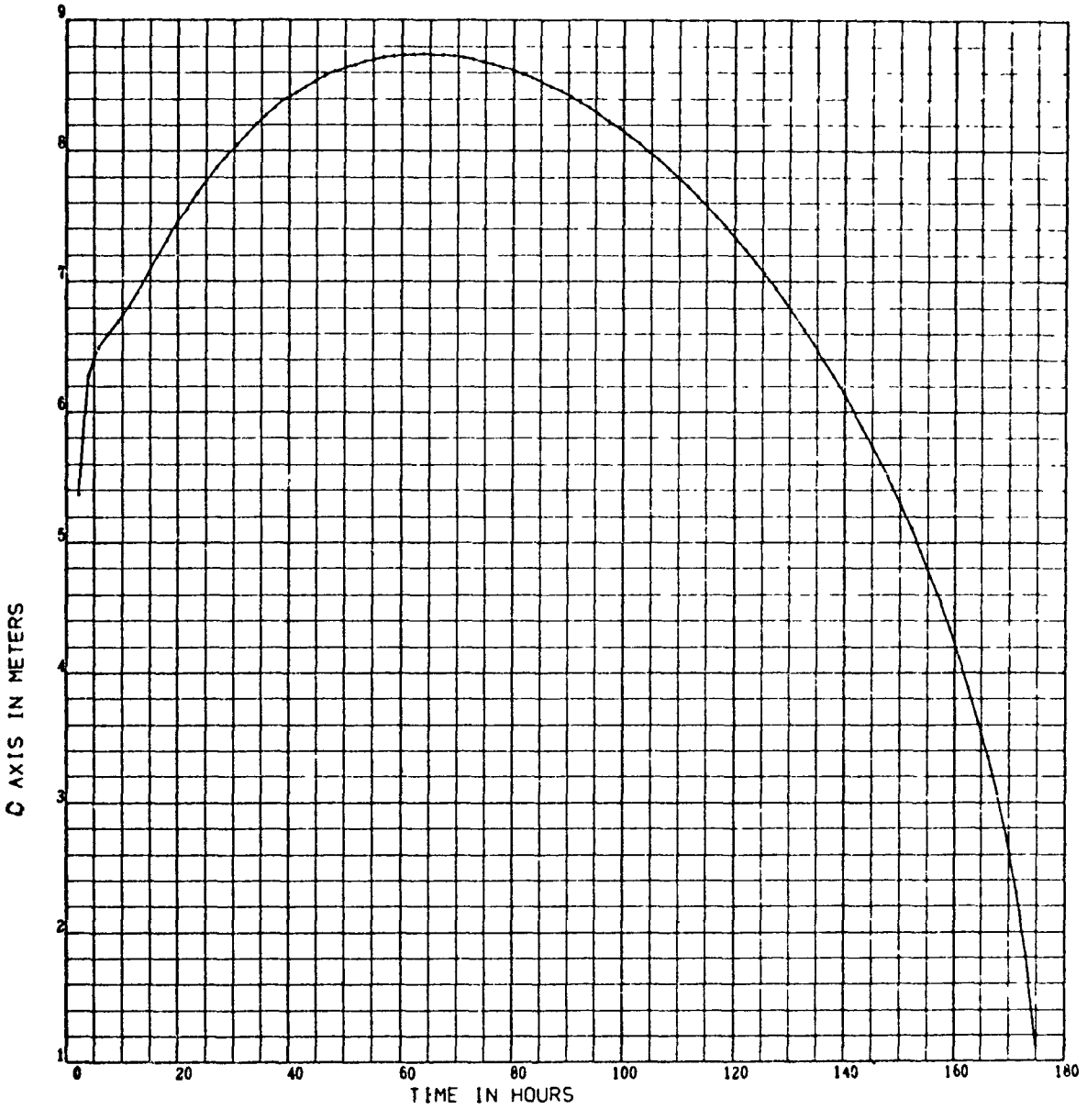

Figure 4(c). Computer Plotted Output for Ellipsoid Semi-Axis(C) vs. Time

TABLE 9

CHARACTERISTICS OF MAXIMUM VOLUME ELLIPSOIDS
(Instantaneous Release)

Parameter	Multi-* Factor	t_{max}, Hrs.		T, Hrs.		V_{max}, m^3		Semi-Axis, m					
								a		b		c	
		0.5 KW	1 KW	0.5 KW	1 KW	0.5 KW	1 KW	.5 KW	1 KW	.5 KW	1 KW	.5 KW	1 KW
Standard**		96	127	175	231	6.76×10^8	13.5×10^8	21,700	33,000	900	1,030	8.26	9.47
Ω_y=2.38	--	48	64	88	116	"	"	43,000	65,600	335	384	11.20	12.82
Ω_y=23.8	--	19	26	35	46	"	"	106,000	165,000	204	231	7.45	8.46
Ω_y=119.0	--	10	13	18	24	"	"	203,000	304,000	147	170	5.40	6.23
Ω_y=238.	--	8	10	14	18	"	"	277,000	405,000	126	147	4.62	5.40
Ω_y=2380.	--	3	4	5	7	"	"	1.05×10^7	1.53×10^7	78	93	1.97	2.26
Ω_z=0.0	0	507	806	1379	2171	"	"	2,066	2,600	2,066	2,600	37.8	47.6
Ω_z=2.38	.1	237	315	437	579	"	"	8,500	13,000	1,411	1,630	13.4	15.2
Ω_z=119	5	51	67	92	121	"	"	41,700	63,000	650	748	5.96	6.85
Ω_z=238	10	38	51	69	92	"	"	54,400	83,400	569	650	5.21	5.95
Ω_z=2380	100	15	20	27	36	"	"	136,000	208,000	360	412	3.30	3.77
A_x=14.	.01	96	127	175	231	"	"	21,700	33,000	900	1,030	8.20	9.46
A_x=140	.1	96	127	175	231	"	"	21,700	33,000	900	1,030	8.25	9.46
A_x=7,000	5	96	127	175	231	"	"	21,700	33,000	895	1,030	8.30	9.50
A_x=14,000	10	95	126	174	230	"	"	21,600	32,700	894	1,030	8.39	9.56
A_x=140,000	100	85	118	168	226	"	"	19,900	31,200	844	995	9.59	10.41
A_y=14	.01	242	319	440	581	"	"	86,800	131,000	142	164	13.06	15.0
A_y=140	.1	153	201	277	366	"	"	43,600	65,800	358	411	10.36	11.9
A_y=7,000	5	70	92	127	167	"	"	13,400	20,300	1,713	1,970	7.02	8.07
A_y=14,000	10	61	80	110	145	"	"	10,860	16,400	2,268	2,610	6.56	7.45
A_y=140,000	100	38	50	69	92	"	"	5,213	7,530	5,890	7,120	5.26	6.02
A_z=.0047	.01	605	800	1095	1445	"	"	31,500	47,800	2,466	2,840	2.08	2.38
A_z=.047	.1	242	319	440	581	"	"	27,200	41,200	1,434	1,649	4.14	4.75
A_z=2.35	5	51	67	92	121	"	"	18,700	28,200	649	747	13.3	15.3
A_z=4.7	10	38	51	69	92	"	"	17,200	26,400	568	647	16.5	18.8
A_z=47	100	15	20	27	36	"	"	13,600	20,800	360	412	33.0	37.8

*Multiplication Factor
**See Table 8 for values of standard parameters

The volume (V) was expressed analytically as a function of time, differentiated with respect to time, and the derivative set equal to zero to obtain t_{max}. Resubstitution of t_{max} in the volume expression gives:

$$V_{max} = \frac{4\, M_o\, e^{-3/2}\, \sqrt{27/8}}{3\pi^{1/2}\, D_o} = \text{constant} \qquad (29)$$

for M_o = 74,600 Ci of Sr^{90} oxide

D_o = 1 MPCC = 3.4×10^{-5} Ci/m^3

V_{max} = 6.76×10^{8} m^3

which is the same result obtained from the NRDL instantaneous digital computer code (Table 9).

As a result of the parametric study summarized in Table 9 the following general concludions were drawn.

1. The maximum volume contained within a given isoconcentration surface is independent of the empirical constants in the Carter-Okubo transport equation.

2. The amount of time required to reach a maximum volume and the time during which concentration greater than or equal to the specified MPCC level persist are sensitive to the values used for the empirical constants.

3. The empirical constants affect the overall shape of the ellipsoidal volume.

Other more specific conclusions which depend upon the range chosen for the empirical constants in the standard comparison case may also be observed from Table 9.

1. The eddy diffusivity in the x direction (A_x) is the most insensitive parameter.

2. The horizontal shear, Ω_y which was taken approximately as zero in the standard case, will affect the major axis of the ellipsoid more than any other parameter.

3. The vertical shear, Ω_z, affects the time duration of the radioactive pool more than any of the other empirical constants.

4. Changes in A_y produce a strong effect on the b semi-axis, which approximately coincides with the y-axis.

5. Changes in A_z produce a strong effect on the C semi-axis, which approximately coincides with the Z-axis.

The effects of these diffusion parameters on marine radio-contamination will be discussed in Section IV.2.

III.3.4.3 Continuous Release

Although the continuous digital computer code has not been fully completed it has been possible to calculate the volume and dimensions of the contaminated pool. These results are obtained after the quasi-steady state conditions, previously discussed, have been achieved. The contaminated water pool will hence remain at a fixed location in the ocean for a prolonged period of time (years) due to the slowly dissolving $^{90}SrTiO_3$ fuel.

Figure 5 presents the results obtained for a 7.46×10^4 Ci $SrTiO_3$ source. The following observation may be made from this figure.

1. The quasi-steady times are less than one hour for the continuous case.

2. The volumes contained within isoconcentration contours are much smaller for the continuous solution than they are for the corresponding instantaneous solution.

3. The ellipsoidal shape of the isoconcentration surfaces are very slightly irregular for the continuous solution.

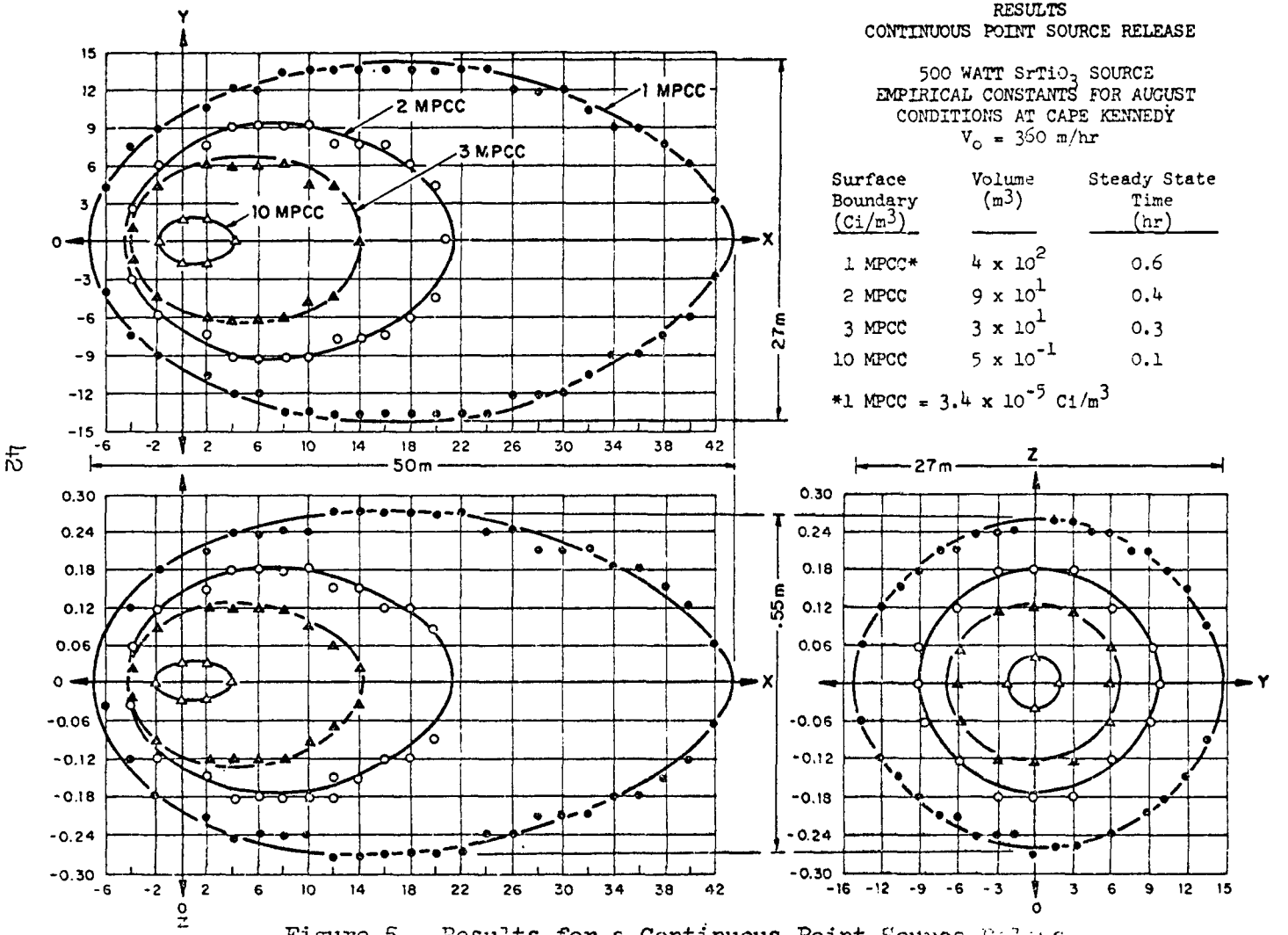

Figure 5. Results for a Continuous Point Source Release

IV. BIOLOGICAL IMPLICATIONS OF THE INSTANTANEOUS RELEASE OF ^{90}Sr-OXIDE INTO CALIFORNIA COASTAL MARINE ENVIRONMENT

This part of the study complements the ocean diffusion analysis developed under Section III.3. Its main objective was to estimate the level of contamination among certain important marine biota resulting from an instantaneous release of 7.46×10^4 curies of ^{90}Sr (a 500 watt source of ^{90}SrO). Vaughan[2] carried out this study for California coastal waters, a typical environment where a marine radioisotopic generator might be used for example to power acoustic devices for navigational purposes. This section summarizes Vaughan's work[2] and includes results of a parametric study completed by the authors using Vaughan's Migratory Marine Organism Contamination Model.

IV.1 Summary of Biological Effects on California Marine Organisms

1. The yearly catch of fish and shellfish in California in 1965 amounted to about 84 million Kg, of which 21 million Kg were benthic organisms. The balance consisted of pelagic filter-feeders and carnivores. For this majority, typical radiostrontium concentration factors are as follows:

Bone	200
Scales	10
Viscera	1
Muscle	0.3

2. Most of the catch is eaten directly. A small but not negligible fraction is used in processing fish meal and fish protein concentrate. Menhaden, tuna, mackerel, herring and sardine (all pelagic) comprise the bulk of fish used for this purpose. Radiostrontium is readily exchangeable in most of the soft tissue of these fishes. This is not the case, however, with mineralized tissues which comprise about 10% of the total body weight.

Although bone concentration factors may be as high as 200, bone contamination level is not expected to exceed that of the soft tissue due to the limited duration of the contaminated pool in the instantaneous release case (as can be seen in Section III.3 above).

3. The amount of kelp harvested per year is estimated to be 56 million Kg. Seaweeds such as kelp concentrate radiostrontium significantly achieving equilibrium concentration in a few days. Their concentration factors vary from 3 to 27. The commercial interest in seaweeds is the extraction of alginic acid and alginates from Macrosystic (kelp) and agar from Gelidium cartilagineum (red algae).

During the extractive processes one may estimate that at least 90% of the ^{90}Sr will be eluted, based on binding studies in this Laboratory on the green algae, Ulva.

4. The amount of radioelement (R_f) taken up by a marine organism can be calculated as follows:

$$R_f = R(t) \cdot C(t) \cdot F(V_r) \tag{30}$$

where $R(t)$ is the dissemination factor or average concentration of the radioelement within an isoconcentration contour,

$$R(t) = \frac{m(t)}{V(t)} \tag{31}$$

where $m(t)$ is the amount of fuel dissolved and $V(t)$ is the volume of contaminated water within a specified isoconcentration contour,

$C(t)$ is the uptake factor, which for short term accumulation can be described by the equation.

$$C(t) = C_o\ (1-e^{-kt}) \tag{32}$$

where C_o is the concentration factor mentioned under 1. above, k is a constant applicable to soft tissue, and t is the time in days during which the fish is exposed to radioactivity, where duration of the pool is comparatively long.

For most migratory fish and for the zooplankton monitored in Operation Swordfish a value $K = 0.4$ is applicable. This value may not be applicable to sedentary or sessile marine organisms, and it does not necessarily apply to the release of radioelement, which may for some organisms be slower than the uptake. For migratory fish, this kinetic expression will apply to at least 90% of ^{90}Sr taken up.

$F(V_r)$ is the interception fraction based on the fraction of time fish spend in radioactive water.

$$F(V_r) = \frac{V(t)}{V_f} \tag{33}$$

where V_f is the fish migratory volume, taken as the volume of a cube of a side equal to the daily migration distance. It is assumed here that fish swim in a random search pattern, in and away from shore, with a net daily shift in location. Small pelagic species show a migratory range of about 5 miles per day. Tuna and other large, ocean going carnivores show a migratory range of 15 to 25 miles per day typically. For conservative estimation, these fishes can be grouped with the small pelagic species, so all migratory species are assigned a 5 mile/day migratory range.

The interception fraction is assumed to be unity when the volume of the radioactive pool equals or exceeds the daily migratory volume. Analysis of the data obtained from biological samplings during Operation Swordfish yielded an $F(V_r)$ value of 0.6 for zooplankton. The radioactive pool size was larger than any reasonable migratory volume in this case.

The three parameters in equation (30) above were calculated by Vaughan to estimate radiocontamination in soft tissue of pelagic fish (R_f) resulting from an instantaneous release of 7.46×10^4 Ci of $^{90}Sr0$. Volumes of contaminated water pools and amounts of activity contained within isoconcentration contours were calculated by the instantaneous release model described under Section III.3 above. Two points in time were chosen; 7 hrs and 24 hrs post release. Table 10 presents the results obtained. Examination of the data in this table reveals the following:

1. R_f is independent of the average concentration (R). Higher values of R across inner shells are approximately offset by lower interception fraction for these smaller pools.

2. R_f for 24 hours is about 3 times higher than its value for 7 hours as a consequence of the three-fold increase in residence time of fish in the radioactive pool.

3. Radiocontamination levels in the migratory fish are negligibly small in relation to the water contamination level (=82 cpm/cm^3 water for 1 MPCC), and they would remain so even if the pool duration lasted long enough for 100% uptake.

Four conditions should be carefully considered in the event this model for short-term exposure of migratory organisms were to be generalized:

a) Ocean-going carnivores like tuna, because of their longer daily migratory distance, should show lower contamination levels;

TABLE 10*

RADIOCONTAMINATION IN SOFT TISSUE OF PELAGIC FISH

Isoconcentration Contour, MPCC	Volume of Contaminated Water, cm^3	Percentage of Radioactivity With the Contour	Average Concentration Within Contour, dpm/cm^3 R	Interception Fraction** F	Uptake Factor C	Radioactivity in Tissue dpm/gm R_f = R.F.C.
At 7 hrs post release						
1	17×10^{12}	99.	0.97×10^{4}	33×10^{-6}	0.033	1×10^{-2}
10	10	98.	1.6	20	"	1
100	4.2	89.	3.5	8.2	"	1
1000	0.5	31.	10.4	2.5	"	1
At 24 hrs post release						
1	13×10^{12}	98.	1.3×10^{4}	25×10^{-6}	0.099	3×10^{-2}
10	5.1	85.	2.8	10	"	3.
100	2.1	11.	0.9	4.1	"	0.3
1000	0	-	-	-	-	

*Copied from reference 3

**Assuming a migratory range of 5 miles

b) Benthic organisms like crab should show higher contamination levels, if they lie within the geographical boundaries of the pool, but outside these boundaries they should show no radioactive contamination, because of their highly localized migratory activity;

c) Sessile organisms such as seaweeds similarly cannot be expected to show significant radiocontamination if they lie outside the geographical boundaries of the pool at its maximum extent; inside the pool they will be contaminated significantly but to an indefinite magnitude;

d) the radiocontamination model, in common with any in use, is probabilistic in the sense that a few of the migratory fish to which it is applicable may show higher or lower radioactivity because of variations from typical migratory patterns; i.e., a few may remain wholly inside the pool, and some other may remain wholly outside.

IV.2 Effect of Diffusion Parameters on Radiocontamination in Soft Tissue of Pelagic Fish

Under Section III.3.4.2 it was observed that varying the empirical diffusion parameters resulted in changes of the time duration and physical dimensions of the contaminated pool. This section of the report evaluates the effect of these changes on marine radiocontamination as calculated by the Migratory Marine Organism Contamination Model presented in Section VI.1. Since the major objective of this parametric study was to determine the sensitivity of the model, the range of values used for the empirical constants does not necessarily reflect what might be realistically measured in California coastal waters. The parameters used for the standard case (see Table 8) were measured in the coastal waters near Cape Kennedy, and were used by Vaughan in obtaining the values appearing in Table 10 of Section IV.1.

In evaluating the marine radiocontamination model a time averaged amount of radioactivity in the soft tissue of pelagic fish, $\bar{R}_f$, was calculated. The authors consider $\bar{R}_f$ to be more meaningful than R_f calculated in Section IV.1. In the case of R_f the calculation is made for a specific time which to some extent is arbitrary (for example 7 hours in Section IV.1). In $\bar{R}_f$ the amount of radioactivity is averaged over the duration of the radioactive pool, T, as follows:

$$\bar{R}_f = \frac{1}{T} \int_0^T F(V_r)\, R(t)\, C(t)\, dt \qquad (34)$$

It may be observed from Table 11 that the value for $\bar{R}_f$ in th standard case (.032 dpm/gm) is greater than R_f at 7 hours (0.01 dpm/gm)* but approximately equal to R_f at 24 hours (0.03 dpm/gm).*

Examination of Table 11 leads to the following conclusions:

1. A_z is the most effective parameter in terms of the marine radiocontamination.

2. A_y is very insensitive.

3. The values calculated for $\bar{R}_f$ are nonlinear with source strength.

4. Although the diffusion parameters affect the dimensions and time duration of the radioactive pool the effect of these parameters on $\bar{R}_f$ is relatively small. In the case under consideration a factor of less than 7 may be observed over the full A_z range.

*See Table 10 of Section IV.1

TABLE 11

EFFECT OF DIFFUSION PARAMETERS ON RADIOCONTAMINATION IN SOFT TISSUE OF PELAGIC FISH

Parameter Varied	Multiplication Factor	T in Hours		$\bar{R}_f$, dpm/gm	
		.5 KW	1 KW	.5 KW	1 KW
Standard	1	175	231	0.032	0.074
$\Omega_y = 2.38$	-	88	116	0.021	0.051
$\Omega_y = 23.8$	-	35	46	0.010	0.026
$\Omega_y = 119$	-	18	24	0.0058	0.015
$\Omega_y = 238$	-	14	18	0.0044	0.012
$\Omega_y = 2380$	-	5	7	0.0018	0.0048
$\Omega_z = 0.0$	0	1379	2191	0.041	0.084
$\Omega_z = 2.38$	.1	437	579	0.045	0.096
$\Omega_z = 119$	5	92	121	0.022	0.052
$\Omega_z = 238$	10	69	92	0.018	0.043
$\Omega_z = 2380$	100	27	36	0.0083	0.021
$A_x = 14$	.01	175	231	0.032	0.074
$A_x = 140$	.1	175	231	0.032	0.074
$A_x = 7,000$	5	175	231	0.032	0.074
$A_x = 14,000$	10	174	230	0.032	0.074
$A_x = 140,000$	100	168	226	0.029	0.069
$A_y = 14$	.01	440	581	0.046	0.097
$A_y = 140$	.1	277	366	0.039	0.087
$A_y = 7,000$	5	127	167	0.027	0.064
$A_y = 14,000$	10	110	145	0.025	0.058
$A_y = 140,000$	100	69	92	0.018	0.043
$A_z = .0047$	.01	1095	1446	0.053	0.109
$A_z = .047$	.1	440	581	0.046	0.097
$A_z = 2.35$	5	92	121	0.022	0.052
$A_z = 4.7$	10	69	92	0.018	0.044
$A_z = 47$	100	27	36	0.0083	0.021

V. CONCLUSIONS AND RECOMMENDATIONS FOR ADDITIONAL AREAS OF INVESTIGATION

V.I CONCLUSIONS

The following general conclusions can be drawn from the analyses presented in this report:

1. The physico-chemical characteristics of ^{90}SrO and $^{90}SrTiO_3$ cannot, alone, serve as a basis for preference of one over the other as a fuel for terrestrial/marine radioisotopic power units.

2. Replacing the titanate with an oxide-fueled unit of the same power saves about 20% of the component materials for a typical radioisotopic unit.

3. An unshielded intact ^{90}SrO fuel capsule delivers 1.06 to 1.5 times higher doses than an equivalent $^{90}SrTiO_3$ capsule.

4. Skin doses from oxide particles are higher by a factor of 1.76 than those from titanate particles of equal weight and by a factor of 1.62 than those of equal size particles.

5. The hazard to the bone from oxide particles dissolved in the GI tract is 1.6 to 72 fold higher than that from titanate particles of the same size, depending on the particle size and GI transit time. On the other hand, even the smallest titanate particle is capable of delivering, in a matter of hours, doses in excess of 15 rems (the maximum allowable yearly dose) to a limited area of tissue if it settles on the GI epithelial lining. This problem does not exist with the (soluble) ^{90}SrO particles.

6. The maximum allowable yearly dose to the GI tract can be exceeded from a titanate particle of a smaller size than that of an oxide particle necessary to supply the maximum permissible bone burden of ^{90}Sr.

7. A titanate particle of the maximum size deposited in the deep lung delivers about 0.2 rads of β dose to the lung while dissolving. When dissolved (in a little over a day) it would have delivered about 56% as much ^{90}Sr to the different organs of the body as would have an oxide particle of equal size.

8. Using the empirical diffusion parameters for August conditions at Cape Kennedy, the Carter-Okubo diffusion model predicts that for an instantaneous point source release of 7.46×10^4 Ci of ^{90}SrO the maximum volume contained within a 1 MPCC isoconcentration surface will be 6.76×10^8 m^3. The dimensions of the semi-axis of this maximum ellipsoid are 21,700 m, 900 m and 8 m. The total time duration of the 1 MPCC

radioactive pool is 175 hours. On the other hand the model predicts that for a continuous release of $^{90}SrTiO_3$, from an initial fixed point source of 7.46×10^4 Ci, there will be a steady state 1 MPCC bounded ellipsoid volume of 400 m^3 with semi-axis dimensions of 25 m, 13 m and 0.25 m. This steady state volume is arrived at in less than one hour and will last for 64 years. It may hence be concluded that a ^{90}SrO release would result in a relatively large contaminated pool which will last for a short period of time while a $^{90}SrTiO_3$ release would result in a much smaller pool which would prevail for a longer time.

9. Variation of the empirical diffusion parameters, in the Carter-Okubo model, resulted in changing the time duration and physical dimensions of the contaminated pool. The magnitude of the values obtained for the time duration of the pool ranged from 3 hours to 2,190 hours. For example the semi-axis of a 7.46×10^4 Ci ^{90}SrO source dimensions ranged from 1.05×10^7 m to 5,213 m, from 5,890 m to 78 m, and from 37.8 m to 1.97 m along the approximate x, y and z axis respectively.

10. Based on an NRDL Migratory Marine Organism Contamination Model, the radiocontamination levels in the migratory fish resulting from an instantaneous release of 7.46×10^5 Ci (500 W(t)) of ^{90}SrO are negligibly small in relation to the water contamination level for typical radioactive pool duration times, and they would remain so even if the pool lasted long enough for 100% uptake.

11. Although the diffusion parameters affect the dimensions and the duration of the radioactive pool, the effect of these parameters on the Migratory Marine Organism Contamination Model was relatively small. The time averaged amount of radioactivity was found for example to range from 0.0083 dpm/gm to 0.053 dpm/gm when the eddy diffusivity in the vertical direction was varied over 4 orders of magnitude.

V.2 RECOMMENDATIONS FOR ADDITIONAL AREAS OF INVESTIGATION

In the course of this study several questions were raised that are beyond the state of the art in this field and therefore could not be adequately answered. A brief description of the experimental as well as theoretical studies that should be conducted, if such answers are desired, follows:

1. The Carter-Okubo transport equation used in developing both the instantaneous and continuous models assumes an infinite ocean environment. This environment is never fully realized because of boundry effects at the sea surface, thermocline, or bottom. This assumption is justified because the vertical dimension of the patch

is small, with respect to the horizontal dimensions. However, in the case of a shallow water release the boundary conditions should be considered. It is hence recommended that a mathematical framework for handling boundary condition problems in a turbulent ocean environment should be developed.

2. The cases of estuaries, rivers, lakes and other nonoceanic bodies of water have not been covered in this report. Insofar as radioisotopic power units may be placed in such environments, studies parallel to this investigation should be conducted.

3. The nature of the ecological relationship between deep sea biota and man's food chain has not received adequate study. Recent work shows that flagellated unicells are abundant at depths of 2000 meters and below. The relation of these unicells to organisms of other trophic levels is not clear. Initially deep sea collecting procedures suitable for preservation of the biota of these and different trophic levels should be developed.

4. On-going work on the absorption of ^{90}Sr on ocean bottom material indicates that the limit of solubility of Sr ions in seawater is about 200 mg/liter. Any excess strontium ions in solution combine with sulphate, carbonate, soluble organic compounds, and possibly other anions to form precipitates. In the presence of ocean bottom material, the Sr ion concentration is reduced further. The data obtained to date indicate that about 25% of the Sr is absorbed.

As to the consequences to the biology of the surroundings, most existing knowledge is based on correlative information, e.g., stimulation of primary productivity in areas of upwelling. The literature should be searched for other approaches. Both microscopic, free-swimming forms and large ocean organisms--which disturb the bottom sediment by burrowing--would be expected to accelerate movement of radioelement from the sedimentary deposit into the water. Laboratory simulation experiments are feasible.

In regard to particulate matter in the pelagic region, particles less than one micron can be expected to adhere by various adsorption mechanisms to the mucilaginous outer coat of many phytoplankton, varying from 1 to 50 microns in size. Larger radionuclide articles will sediment, and some loss of the adsorbed smaller particles will occur by fecal "pellet processing" (by the zooplankton). Laboratory experiments to determine the binding of particulate radionuclide by phytoplankton should be carried out.

5. Unlike pelagic species, no hazard evaluation from contaminated shellfish appears in this report. Although determining the uptake of ^{90}Sr in both the edible and unedible portions of shellfish would seem feasible, no studies of this problem are yet available.

6. The effect of the uptake of radiostrontium by a particular branch of animal or plant life on the biological balance has not been evaluated. Meaningful ecosystem models cannot be constructed presently because information is inadequate on specific food webs, representative species are variable, and their numbers are not accurately known. At high activity levels crude estimates of the degree of biological unbalance can be made from existing data. Fish, in particular are quite radiosensitive in early embryonic stages but not later. Apparently authoritative Russian research claims that ^{90}Sr concentration of 10^{-11} to 10^{-12} Ci/liter is critical for the development of sea fish eggs in the hyponeuston layer. To our knowledge, experiments specifically designed to assess alteration in population dynamics of an ecosystem have not been done in the U.S. Even if the Russian findings were true, the volume of contaminated water considered in our study is relatively so small that any effect of radiation on the ecosystem would not be significant.

REFERENCES

1. Berlandi, F. J., Kawahara, F. K., Kim, J. and Schrock, V. E., "Radioisotopic Power Generators: State of the Art Report", U. S. Naval Radiological Defense Laboratory, USNRDL-R&L-68-6, March 1968.

2. Vaughan, B. E. and Strand, J. A., "Biological and Theoretical Implications of an Instantaneous Release of ^{90}Sr-Oxide Into the California Coastal Marine Environment", U. S. Naval Radiological Defense Laboratory, USNRDL-TR-68-18, January 1968.

3. Carter, H. H. and Okubo, A., "A Study of the Physical Processes of Movement and Dispersion in the Cape Kennedy Area," Chesapeake Bay Institute, The Johns Hopkins University, Report No. NYO-2973, March 1965.

4. Mikhail, S. Z. and James, L. R., "Development of the Ocean Diffusion Models", Sandia Corporation, Quarterly Progress Report October 1 to December 31, 1967. Prepared by U. S. Naval Radiological Defense Laboratory. In press.

5. Phase I, Quarterly Progress Report WANL-PR-(SS)-004, March 1 - May 31, 1967, Westinghouse Astronuclear Laboratory, pp. 3-111 to 3-114.

6. Ibid.,.p. 3-9

7. Ibid., pp. 3-121 - 3-125

8. Ibid., pp. 3-117 - 3-120

9. Arnold, E. D., Handbook of Shielding Requirements and Radiation Characteristics of Isotopic Power Sources for Terrestrial, Marine and Space Applications, USAEC Report ORNL-3576, Oak Ridge National Laboratory (April 1964).

10. "Recommendations of the International Commission on Radiological Protection," ICRP Publication 6, 1962.

11. Task Group on Lung Dynamics for Committee II of the International Radiological Protection Commission, "Deposition and Retention Models for Internal Dosimetry of the Human Respiratory Tract," Health Physics 12:173-201, February 1966.

12. "Recommendations of the International Commission on Radiological Protection" ICRP Publication 2, 1959.

13. Report of the International Commission on Radiological Protection, Committee II on Permissible Doses for Internal Radiation (1959); Health Physics 3, 152 (June 1960).

14. Le Roy, G. V., Rust, J. H. and Hasterlik, R. J., "The Consequences of Ingestion by Man of Real and Simulated Fallout," Argonne Cancer Research Hospital, ACRH-102.

15. Hayes, R. L., Carlton, J. E. and Butler, W. R., Jr., "Radiation Dose to the Human Intestinal Tract from Internal Emitters," Health Physics, 9, 915 (1963).

16. Smith, D., "Comparison of Theoretical Ocean Diffusion Models," USNRDL-TR-67-50 (May 1967).

17. Korn and Korn, "Mathematical Handbook for Scientists and Engineers," McGraw Hill, 1961.

18. Carslaw and Jaeger, "Conduction of Heat in Solids", Oxford Press, 1959.

19. "The Relative Hazards of Two RTG Fuels; ^{238}Plutonium Dioxide and ^{90}Strontium Titanate", Sandia Corporation Report in Press.

APPENDIX A

CHARACTERISTICS OF THE STRONTIUM-90 TITANATE-FUELED RADIOISOTOPIC GENERATORS

TABLE A-I

STRONTIUM TITANATE-FUELED RADIOISOTOPIC GENERATORS

Generator	Amount of Fuel	Total Weight	Design Electrical Output	Design Life	POWER SYSTEM				THERMOELECTRICS				Encapsulant	Biological Shield
					Voltage	Thermal Output	Electrical Output	Efficiency	Material	No. of Couples	H. J. Temp.*	C. J. Temp.**		
SENTRY	17.5 KCi	1,680 lbs	5 W	2 yrs	3.5-4V	117 W	4.2 W	3.6 %	PbTe	60	453°C	53°C	Hastelloy C	Cast lead
SNAP-7A	40.8 KCi	1,870 lbs	10 W	2 yrs	6 V	256.5 W	10 W	2.6 %	PbTe	60	482°C	65°C	Hastelloy C	Uranium
SNAP-7B	225 KCi	4,600 lbs	60 W	10 yrs	10 V	1410 W	60 W	4.3 %	PbTe	120	535°C	93°C	Hastelloy C	Uranium
SNAP-7C	40 KCi	1,840 lbs	10 W	2 yrs	5 V	256 W	10 W	2.6 %	PbTe	/	493°C	/	Hastelloy C	Uranium
SNAP-7D	224 KCi	4,600 lbs	60 W	2 yrs	10 V	1410 W	60 W	4.3 %	PbTe	120	535°C	93°C	Hastelloy C	Uranium
SNAP-7E	31 KCi	6,000 lbs	7.5 W	2 yrs	4.5 V	198 W	7 W	3.5 %	PbTe	60	437°C	143°C	Hastelloy C	Cast Iron
SNAP-7F	225 KCi	4,600 lbs	60 W	10 yrs	/	/	60 W	/	PbTe	120	535°C	93°C	Hastelloy C	Uranium

* Hot Junction Temperature
** Cold Junction Temperature
/ Classified or nor available

TABLE A-I (Cont'd)

STRONTIUM TITANATE-FUELED RADIOISOTOPIC GENERATORS

Generator	Amount of Fuel	Total Weight	Design Electrical Output	Design Life	POWER SYSTEM				THERMOELECTRICS				Encapsulant	Biological Shield
					Voltage	Thermal Output	Electrical Output	Efficiency	Material	No. of Couples	H. J. Temp.*	C. J. Temp.**		
SNAP-17A	≠	10 lbs	10 W	3-5 yrs	≠	≠	≠	≠	≠	≠	≠	≠	≠	≠
SNAP-17B	≠	10 lbs	10 W	3-5 yrs	≠	≠	≠	≠	≠	≠	≠	≠	≠	≠
SNAP-21	30 KCi	507 lbs	10 W	5 yrs	24 V	187 W	12.6 W At BOL≠	6.7 %	PbTe	≠	565-730°C	5-93°C	Hastelloy C	U-8% Mo
SNAP-23*	185 KCi	1000 lbs	60 W	10 yrs	24 V	##	##	##	##	##	##	##	##	##
RIPPLE III**	3.4 KCi	600 lbs	0.71 W	5 yrs	3.1-3.4 V	29 W	0.71-0.80 W	2-5 2.8 %	Bi_2Te_3	2 modules 50 each	235°C	47°C	DELORO alloy "C"	GEC (Tungsten Alloy)
MILLIWATT 3000	20 KCi	2,800 lbs	2.5 W	5 yrs	4.3 V	≠	2.5 W	≠	Bi_2Te_3	192	215°C	51°C	Hastelloy C	Steel, outer Tungsten, inner
LCG-25A	100 KCi	3,000 lbs	25 W	5 yrs	2.6 V	680 W	25 W	3.7 %	PbTe	28	490°C	115°C	Hastelloy C	Tungsten Alloy
LCG-25B	100 KCi	3,000 lbs	25 W	5 yrs	← Same as LCG-25A →									
AGN (URIPS)	6.9 KCi	800 lbs	1 W	5 yrs	24 V	46 W	1 W	2.2 %	Bi_2Te_3	72	204°C	23°C	Hastelloy C	Uranium (or lead)
AI (3 Watt)	≠	250-1,500 lbs	3 W	5 yrs	≠	≠	≠	≠	SiGe	≠	590°C	93°C	≠	≠

*See Table A-III
**See Table A-IV
≠Classified or not available
##System under development
≠Beginning of life

TABLE A-II

TERRESTRIAL SNAP GENERATOR PERFORMANCE ANALYSES*

Generator	Power w(e)		Hours of Operation	Kw-hours[b]
	Design	Average[a]		
1. Project Sentry	4.7	3.9	43,800	171
2. SNAP 7A	10	7.8	39,400	308
3. SNAP 7B	60	56	29,160	1,650
4. SNAP 7C	10	7.8	41,600	346
5. SNAP 7D	60	57	35,000	2,000
6. SNAP 7E	7	6.6	25,000	231
7. SNAP 7F	60	57	14,000	800
TOTALS	--	--	237,960	5,506

* Morse, J. G., Proceedings of the Isotopic Power Generation Conference, Paper No. 21, Harwell, England, September, 1966.

[a] Time average--date of fueling to 1 May 1966.

[b] Based on the time average.

TABLE A-III

CHARACTERISTICS OF SNAP-23 SYSTEMS*/

SYSTEM CHARACTERISTICS	NOMINAL POWER LEVEL							
	10W		25W		60W		100W	
	BOL ≠	EOL ≠≠	BOL	ECL	BOL	EOL	BOL	EOL
Operating Characteristics								
Heat Source Thermal Power (w)	214	167	500	390	1168	910	1830	1430
Heat Losses (w)	49	37	90	66	179	129	200	130
Heat to T/E Converter (w)	165	130	410	324	989	781	1630	1300
Electrical Output (w)	13	10	33	23	79	60	130	100
Heat Rejected by Radiator (w)	152	120	377	299	910	721	1500	1200
Overall Efficiency (%)	6.15	6.0	6.54	6.4	6.75	6.6	7.1	7.0
Thermal Efficiency (%)	77.2	78.0	82	83	84.7	86	89	91
Converter Efficiency (%)	7.97	7.7	7.97	7.7	7.97	7.7	7.97	7.7
Avg. T/E Hot Junction Temp (^{o}F)	1075	880	1075	880	1075	880	1075	880
Avg. T/E Cold Junction Temp (^{o}F)	210	180	210	180	210	180	210	180
Load Voltage (v)	10	10	24	24	24	24	24	24
Load Current (amps)	1.3	1	1.38	1.04	3.28	1.25	5.41	4.16

*"SNAP-23A, Data for Terrestrial and Marine Systems Applications", AEC, January, 1967.

/Design Specifications--systems are presently under development.

≠Beginning of life

≠≠End of life

TABLE A-III (Cont'd)

CHARACTERISTICS OF SNAP-23 SYSTEMS*/

SYSTEM CHARACTERISTICS	POWER LEVEL							
	10W		25W		60W		100W	
Overall Diameter (in.)	18		20		24		28.625	
Overall Height (in.)	17.5		20.625		25.85		28	
Design Life (yr.)	5	10	5	10	5	10	5	10
System Weight (lbs.)	490	531	686	706	1010	1040	1810	1898

*"SNAP-23A, Data for Terrestrial and Marine Systems Applications", AEC, January, 1967.

/Design Specifications--Systems are presently under development.

TABLE A-IV

CHARACTERISTICS OF RIPPLE GENERATORS*

RIPPLE	I(a)	I(b)	II(a)	II(b)
Isotope	Sr^{90}	Sr^{90}	Sr^{90}	Sr^{90}
Fuel Form	Titanate	Titanate	Titanate	Titanate
Quantity	600 curies	700 curies	700 curies	700 curies
Canning	Stainless Steel	Stainless Steel	Stainless Steel	Stainless Steel
Thermal Power	3.75 watts	4.4 watts	4.4 watts	4.4 watts
Electric Power	52 mW	75 mW	78 mW	89.6 mW
Efficiency	1.39%	1.7%	1.8%	2.0%
Thermoelements	Bi_2Te_3	Bi_2Te_3	Bi_2Te_3	Bi_2Te_3
Number of Couples	18	18	18	18
Size of Elements	$(1.5mm)^2$ x1cm	$(1.5mm)^2$ x1cm	$(1.5mm)^2$ x1cm	$(1.5mm)^2$ x1cm
Hot Junction Temperature	176°C	180°C	180°C	200°C
Cold Junction Temperature Ambient 20°C	38°C	40°C	40°C	40°C
Volts Open Circuit	0.720	0.994	1.006	1.080
DC-DC Conversion	Ge Tunnel Diodes	Ga As Tunnel Diodes	Ga As Tunnel Diodes	Ga As Tunnel Diodes
Output after Inversion	20 mW	30 mW	30 mW	45 mW
Voltage after Inversion	6	6	6	6
Efficiency of Inversion	38%	42%	42%	45%
Shielding	Lead	Lead	Heavy Alloy	Heavy Alloy
Total Weight	600 kg	600 kg	230 kg	230 kg

*Hane, G. E., "Radioisotope Powered Generator Development in the United Kingdom", AERE, DP-1066, Vol II, March 1966.

APPENDIX B

PHYSICAL, CHEMICAL AND RADIOLOGICAL CHARACTERISTICS OF STRONTIUM-90 METAL, STRONTIUM-90-OXIDE AND STRONTIUM-90 TITANATE

B.1 STRONTIUM-90 METAL*

B.1.1 Composition

a. Abundance of nuclides

Spectrometric analysis of aged fission-product strontium yielded the following data:

^{90}Sr	55%
^{89}Sr	43.9%
^{86}Sr	1.1%

b. Radionuclidic activities

Fission-product strontium, when fresh, contains the following nuclides in addition to ^{90}Sr:

Nuclide	Half Life
^{88}Sr	stable
^{89}Sr	54 days
^{91}Sr	9.7 hours
^{92}Sr	2.7 hours
^{93}Sr	8.3 minutes
^{94}Sr	1.2 minutes
^{95}Sr	0.8 minutes
^{96}Sr	2.5 seconds
^{97}Sr	1.5 second
^{98}Sr	1 second
^{99}Sr	1 second
^{100}Sr	.01 second

*The bulk of the data tabulated was obtained from the "Strontium-90 Data Sheets" by S.J. Rimshaw and S.E. Ketchen. ORNL-4188, December 1967. Data obtained from other sources are so identified.

It is noted that, with the exception of ^{89}Sr, all the isotopes are of short half lives. After a few days post chemical separation of Sr from other fission products the principal radionuclide (in addition to ^{90}Sr) is ^{89}Sr. Figure B-1 shows the ratios of $^{89}Sr/^{90}Sr$ activities after 200 days of irradiation as a function of post irradiation time.

c. Cationic composition

1. Range of composition

Analyses of strontium titanate feed samples of the Fission Products Development Laboratory at Oak Ridge National Laboratory (ORNL) showed the following range of composition:

Cation	Maximum	Minimum
Sr	97	92
Ca	5	2
Ba	2	0.5
Mg	2	0
Zr	0	0

One gram of ^{90}Sr produces an average of 0.0232 g of ^{90}Zr after one year day.

2. Average composition

Sr	95
Ca	3.5
Ba	1.0
Mg	0.5

Other activity contributors:

Isotope	Maximum Percentage of Radioactivity
^{144}Ce	0.03%
^{137}Cs	0.003%

B.1.2 Decay Schemes

Figure B-2 presents the decay schemes of ^{90}Sr and ^{89}Sr.

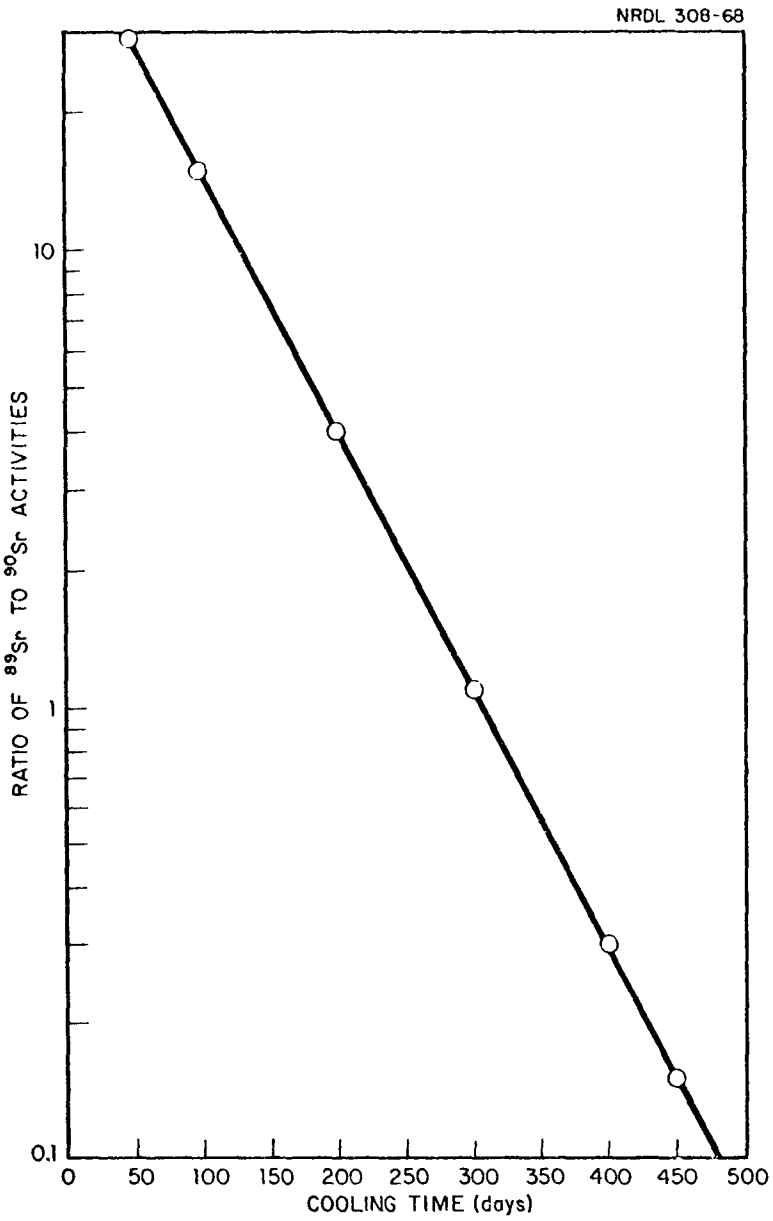

Figure B-1. Ratios of Sr^{89}/Sr^{90} Activities as a function of cooling time post reactor discharge. Irradiation time: 200 days

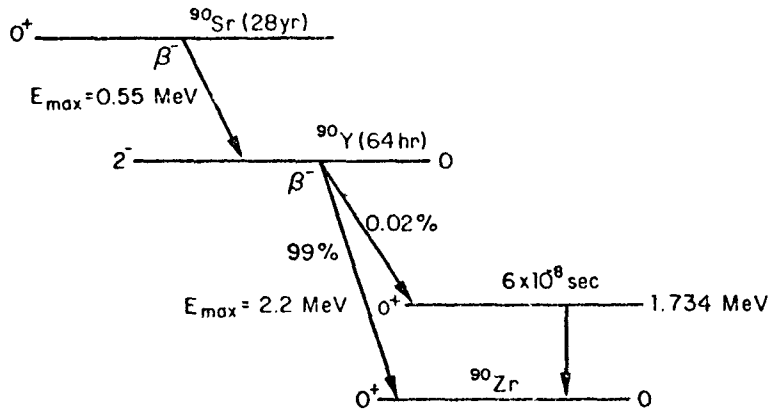

$^{90}Sr - ^{90}Y$

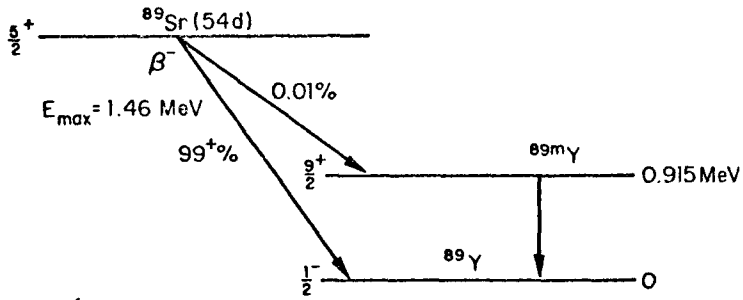

^{89}Sr

Figure B-2. Decay Schemes of ^{90}Sr-^{90}Y and ^{89}Sr

B.1.3 Specific Power

a. 0.963 watt/g of 100% ^{90}Sr (142 curies/g)
b. 0.530 watt/g of pure aged fission product strontium metal (55% ^{90}Sr)
c. 0.503 watt/g of average-composition production quality strontium metal (52.25% ^{90}Sr)

These values do not include ^{89}Sr contribution.

b. 101.66 watt/g of 100% ^{89}Sr (29108 curies/g)

c. Using Figure B-1 and the specific power values reported under a & b the specific power of a $^{89}Sr/^{90}Sr$ fission product mixture can be calculated at different post-chemical separation times.

B.1.4 Radiation (^{90}Sr)

Alpha:	None
Beta:	See Figure B-3
Gamma:	None
Bremsstrahlung:	Intensity and energy of photons produced depend on fuel matrix. For $SrTiO_3$ and SrO matrices see the corresponding sections under those fuel forms.
Neutrons:	None

B.1.5 Compatibility with Materials of Containment

Classified. See USAEC Report ORNL-4189

B.1.6 Thermophysical Properties

a. Density

The theoretical density is 2.6 g/cm^3 for strontium element and 2.55 g/cm^3 for 95% Sr, 3.5% Ca, 1.0% Ba, 0.5% Mg.

b. Coefficient of thermal expansion

$2.0 \times 10^{-5}/^{\circ}C$

c. Specific heat and enthalpy

(1) Specific heat

0.0719 cal g^{-1} $^{\circ}C^{-1}$ ($25^{\circ}C$)

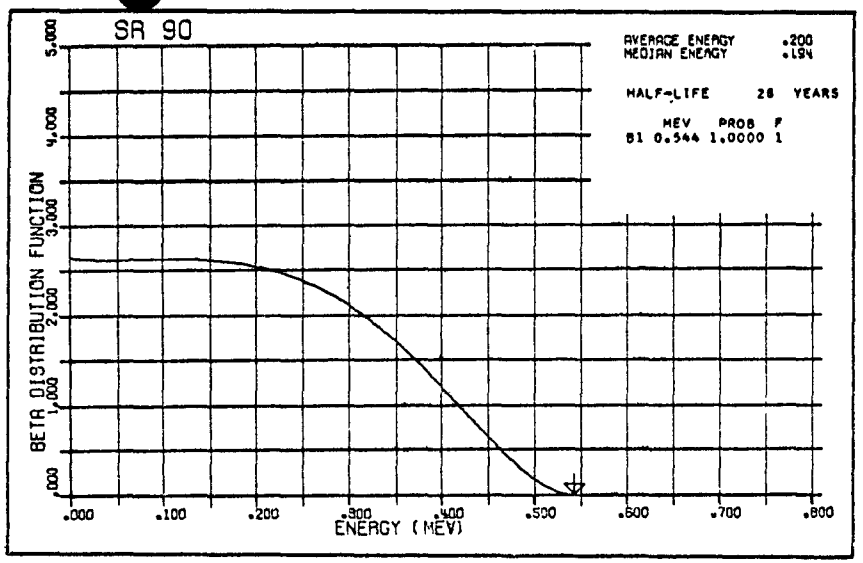

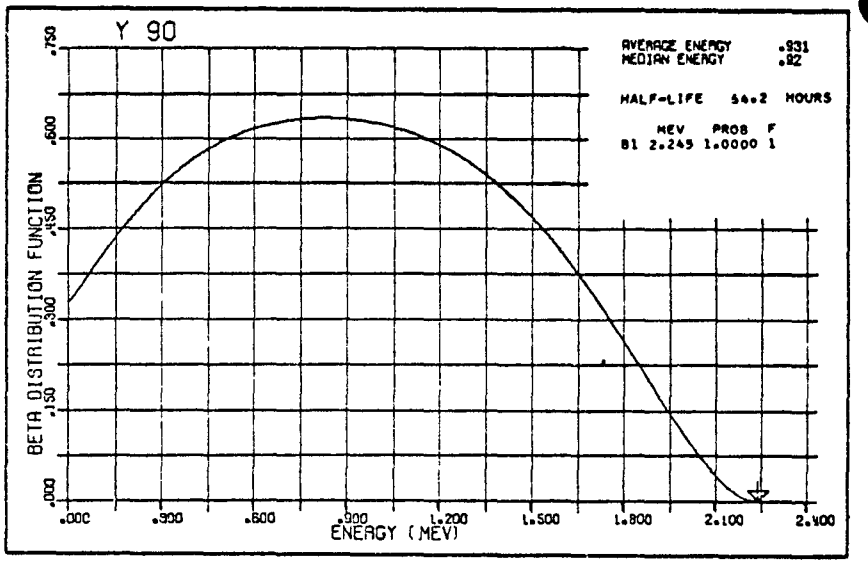

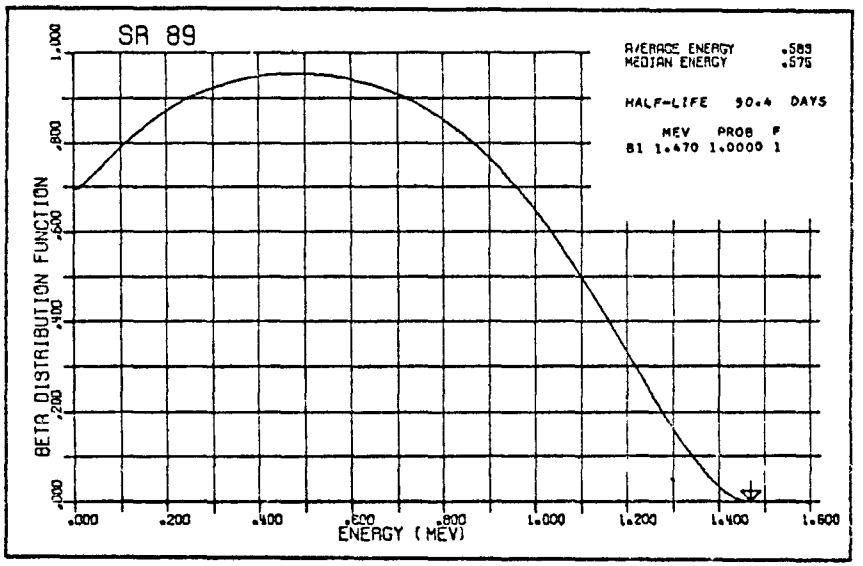

Figure B-3. Beta Spectra of ^{90}Sr, ^{90}Y and ^{89}Sr. (From USNRDL-TR-802 by Hogan, O.K., Zigman, P.E. and Mackin, J.L., 16 December 1964)

(2) Enthalpy in calories/mole

$H_T - H_{298} = 5.31\ T + 1.66 \times 10^{-3}\ T^2 - 1731$ (298-862°K)

$H_T - H_{298} = 9.12\ T - 3582$ (862-1043°K)

ΔH transition = 200 calories/mole at 862°K = 589°C

d. Temperatures of phase transformations

(1) Melting point - 772°C

(2) Boiling point - 1372°C

e. Latent heats of phase transformations

ΔH transition ($\alpha \rightarrow \beta$) = 200 calories/mole (589°C)

ΔH fusion (772°C) = 2400 calories/mole

ΔH vaporization (1372°C) = 33,200 calories/mole

f. Vapor pressure

Atmosphere	Temperature, °C
5×10^{-12}	227
8.7×10^{-4}	727
0.129	1127
0.585	1327
1.9	1527
4.84	1727

g. Thermal conductivity

cal cm^{-1} sec^{-1} $°C^{-1}$	Temperature, °C
0.3	20
0.385	100
0.290	300
0.247	500
0.206	700

h. Thermal diffusivity

cm^2/sec	Temperature, ^oC
1.64	20

This value was calculated by dividing the thermal conductivity by the product of the specific heat and the density.

i. Viscosity

j. Surface tension

σ = 165 dyn/cm

k. Total hemispherical emittance

Varies from 0.25 to 0.80 depending on the state of the sample, such as oxide coating, impurities.

l. Spectral emissivity

Varies also as stated above.

m. Crystallography

α		β		γ
fcc	215°C	hep	605°C	bcc
a = 6.085 Å		a = 4.32 Å c = 7.06 Å		a = 4.85 Å

n. Solubilities

Reacts vigorously with water.

B.1.7 Mechanical Properties

a. Hardness

16-18 (Brinell)

b. Crush strength

B.1.8 Chemical Properties

a. Heat and free energy of formation, entropy

(1) Heat of formation

Zero (standard state)

(2) Free energy of formation

Zero (standard state)

(3) Entropy

S^{o}_{298} = 12.5 eu

b. Chemical reactions and reaction rates

(1) Oxygen - fast

(2) Nitrogen at room temperature - no reaction

(3) Nitrogen at elevated temperature - reacts

(4) Water - reacts

(5) Inorganic acids - reacts

B.1.9 Biological Tolerances

The ^{90}Sr tolerances are given in Table B-I

B.1.10 Shielding Data

See the corresponding sections under $SrTiO_3$ and SrO.

TABLE B-I

MAXIMUM PERMISSIBLE BODY BURDENS AND MAXIMUM PERMISSIBLE CONCENTRATIONS FOR RADIONUCLIDES IN AIR AND IN WATER FOR OCCUPATIONAL EXPOSURE*

Radionuclide and Type of Decay	Organ of Reference (critical organ underscored)	Max. Permissible Burden in Total Body, q(μc)	Maximum Permissible Concentrations, μc/cm³ For 40-hr week		For 168-hr week	
			Water	Air	Water	Air
$38Sr^{90}$ (β^-)	Bone	2	10^{-5}	10^{-9}	4×10^{-6}	4×10^{-10}
	(Sol) Total Body	3	2×10^{-5}	2×10^{-9}	7×10^{-6}	7×10^{-10}
	(Sol) GI (LLI)**		10^{-3}	3×10^{-7}	5×10^{-4}	10^{-7}
	(Insol) Lung			5×10^{-9}		2×10^{-9}
	(Insol) GI (LLI)**		10^{-3}	2×10^{-7}	4×10^{-4}	6×10^{-8}

*Report of the International Commission on Radiological Protection, Committee II on Permissible Doses for Internal Radiation (1959).

**GI. = Gastrointestinal Tract
LLI = Lower Large Intestines

B.2 COMPARISON BETWEEN STRONTIUM TITANATE AND STRONTIUM OXIDE*

STRONTIUM TITANATE	STRONTIUM OXIDE

B.2.1 Composition

a. Abundance of Nuclides

← Same as given in section B.1.1.a for ^{90}Sr metal →

b. Radionuclide Activities

← Same as given in section B.1.1.b for ^{90}Sr metal →

c. Chemical Composition

(1) Range of composition

← Same as given in section B.1.1.c.1 for ^{90}Sr metal
The phase diagram of the $SrO-TiO_2$ system is presented in Figure B-4 →

(2) Average composition

Metal Oxide	Content, wt %	Titanate Compound	Content, wt %
SrO	52.5	$SrTiO_3$	92.5
CaO	2.3	$CaTiO_3$	5.6
BaO	0.5	$BaTiO_3$	0.8
MgO	0.4	$MgTiO_3$	1.1
TiO_2	44.3		

The strontium metal content of pure fission-product $SrTiO_3$ is 48.16%.

The strontium metal content of average fission-product $SrTiO_3$ is 44.55%.

The as-processed $SrTiO_3$ contains 24.5% ^{90}Sr. The ^{144}Ce constitutes 0.03% of the radioactivity at a maximum. The ^{137}Cs has been found to be as high as 0.003% of the total activity. The ^{106}Ru activity has not been found. These activities can be neglected compared to the bremsstrahlung radiation.

Cation	Metal wt, %	Metal oxide, wt %
Sr	95	94.3
Ca	3.5	4.1
Ba	1.0	0.9
Mg	0.5	0.7

The strontium metal content of pure SrO is 84.77%.

The strontium metal content of average SrO is 79.9%.

The as-processed SrO will contain 44.0% ^{90}Sr. The ^{144}Ce constitutes 0.03% of the radioactivity at a maximum. The ^{137}Cs has been found to be as high as 0.003% of the radioactivity at a maximum. The ^{106}Ru activity has not been detected. These activities can be neglected compared to the total radiation.

*The bulk of the data tabulated was obtained from the "Strontium-90 Data Sheets" by S.J. Rimshaw and S.E. Ketchen, ORNL-4188, December 1967. In several cases wording has also been quoted with minor changes. (Data obtained from other sources are so identified.)

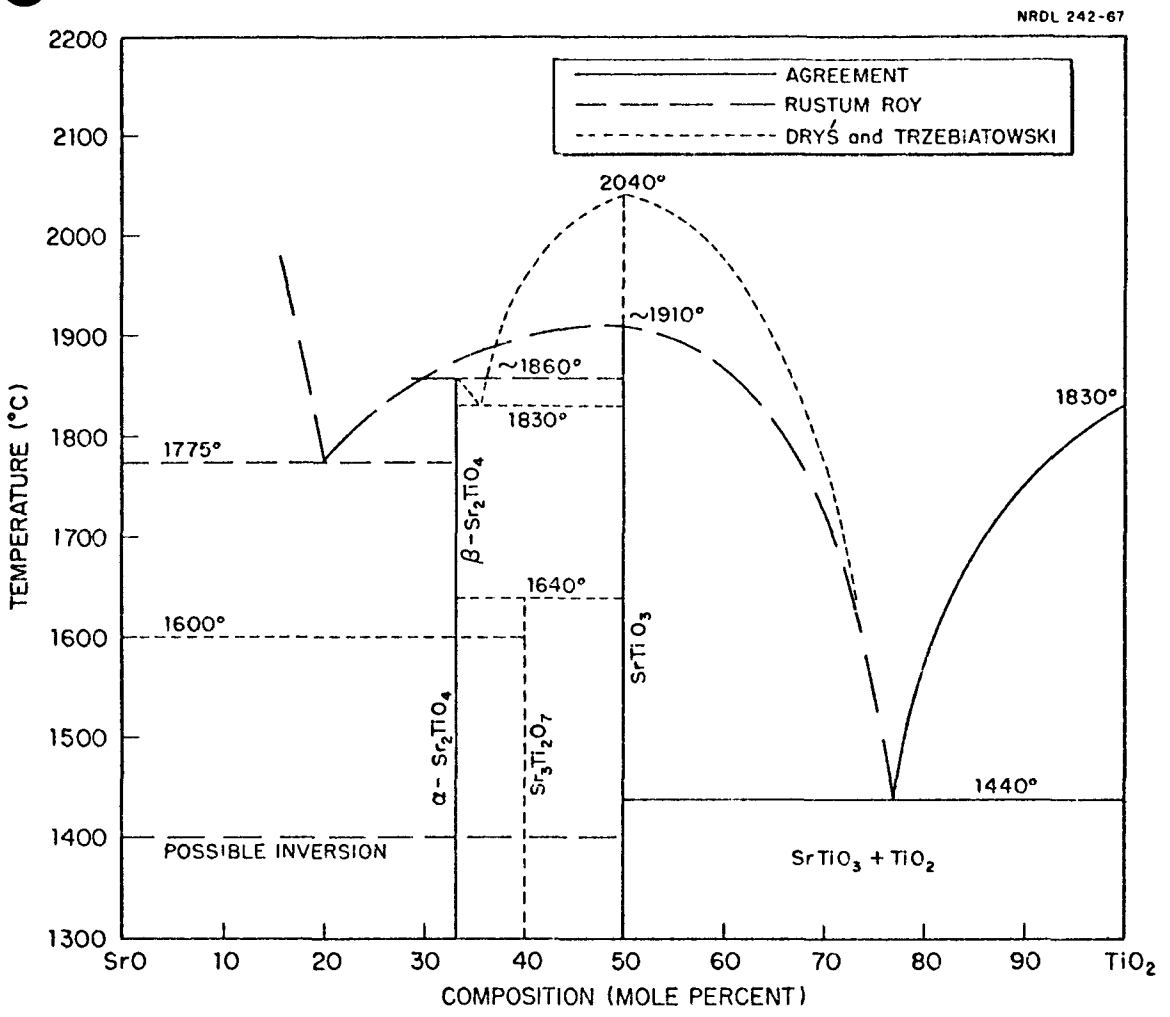

Figure B-4. Phase Diagram of the SrO-TiO_2 System (From USNRDL-LR-67-19 by E. C. Freiling and C. E. Adamas). The figure compounds the data reported by Dry's and Trzebiatowski* with that of Rustom Roy.**

*M. Dry's and W. Trzebiatowski, Roczniki Chem., 31, 492 (1957)
**R. Roy, Private Communication, 1957, cited on p. 119 of E. M. Levin, C. R. Robbins, and H. F. McMurdie, Phase Diagrams for Ceramists, The American Ceramic Society, Columbus, Ohio, 1964.

STRONTIUM TITANATE (Cont'd)

B.2.2 Specific Power

0.2525 watt/g of pure $SrTiO_3$ (26.5% ^{90}Sr metal, 37.6 curies of ^{90}Sr/g)

0.2335 watt/g of average $SrTiO_3$ (24.5% ^{90}Sr metal, 34.8 curies of ^{90}Sr/g)

B.2.3 Radiation

Alpha: None

Beta: See Figure B-3

Gamma: None

Bremsstrahlung:

(1) Photons produced from ^{90}Sr beta in $^{90}SrTiO_3$ Matrix

Bremsstrahlung energy group, Mev	Within ΔE energy group: Photons per beta particle	Photons w^{-1} sec^{-1}
0.020 ± 0.01	1.009×10^{-2}	5.55×10^{10}
0.040 ± 0.01	4.044×10^{-3}	2.22×10^{10}
0.060 ± 0.01	2.195×10^{-3}	1.21×10^{10}
0.080 ± 0.01	1.348×10^{-3}	7.41×10^{9}
0.100 ± 0.01	8.845×10^{-4}	4.86×10^{9}
0.120 ± 0.01	6.034×10^{-4}	3.32×10^{9}
0.140 ± 0.01	4.217×10^{-4}	2.32×10^{9}
0.160 ± 0.01	2.993×10^{-4}	1.65×10^{9}
0.180 ± 0.01	2.141×10^{-4}	1.18×10^{9}
0.200 ± 0.01	1.537×10^{-4}	8.45×10^{8}
0.220 ± 0.01	1.103×10^{-4}	6.07×10^{8}
0.240 ± 0.01	7.871×10^{-5}	4.33×10^{8}
0.260 ± 0.01	5.571×10^{-5}	3.06×10^{8}
0.280 ± 0.01	3.895×10^{-5}	2.14×10^{8}
0.300 ± 0.01	2.678×10^{-5}	1.47×10^{8}

STRONTIUM OXIDE (Cont'd)

0.444 watt/g of pure SrO (46.6% ^{90}Sr metal, 66.2 curies of ^{90}Sr/g)

0.419 watt/g of average SrO (44.0% ^{90}Sr metal, 62.5 curies of ^{90}Sr/g)

Alpha: None

Beta: See Figure B-3

Gamma: None

Bremsstrahlung:

(1) Photons produced from ^{90}Sr beta in ^{90}SrO Matrix

Bremsstrahlung energy group, Mev	Within ΔE energy group: Photons per beta particle	Photons w^{-1} sec^{-1}
0.020 ± 0.01	1.378×10^{-2}	7.58×10^{10}
0.040 ± 0.01	5.523×10^{-3}	3.04×10^{10}
0.060 ± 0.01	2.998×10^{-3}	1.65×10^{10}
0.080 ± 0.01	1.841×10^{-3}	1.01×10^{10}
0.100 ± 0.01	1.208×10^{-3}	0.66×10^{10}
0.120 ± 0.01	8.239×10^{-4}	0.45×10^{10}
0.140 ± 0.01	5.759×10^{-4}	3.17×10^{9}
0.160 ± 0.01	4.086×10^{-4}	2.25×10^{9}
0.180 ± 0.01	2.923×10^{-4}	1.61×10^{9}
0.200 ± 0.01	2.099×10^{-4}	1.15×10^{9}
0.220 ± 0.01	1.505×10^{-4}	0.83×10^{9}
0.240 ± 0.01	1.074×10^{-4}	0.59×10^{9}
0.260 ± 0.01	7.604×10^{-5}	0.42×10^{9}
0.280 ± 0.01	5.315×10^{-5}	2.92×10^{8}
0.300 ± 0.01	3.654×10^{-5}	2.01×10^{8}

Bremsstrahlung energy group, Mev	Within ΔE energy group: Photons per beta particle	Within ΔE energy group: Photons w^{-1} sec^{-1}
0.320 ± 0.01	1.801×10^{-5}	0.99×10^{8}
0.340 ± 0.01	1.179×10^{-5}	6.48×10^{7}
0.360 ± 0.01	7.448×10^{-6}	4.10×10^{7}
0.380 ± 0.01	4.497×10^{-6}	2.47×10^{7}
0.400 ± 0.01	2.559×10^{-6}	1.41×10^{7}
0.420 ± 0.01	1.345×10^{-6}	0.74×10^{7}
0.440 ± 0.01	6.333×10^{-7}	3.48×10^{6}
0.460 ± 0.01	2.534×10^{-7}	1.39×10^{6}
0.480 ± 0.01	7.807×10^{-8}	4.29×10^{5}
0.500 ± 0.01	1.472×10^{-8}	8.10×10^{4}
0.520 ± 0.01	7.336×10^{-10}	4.03×10^{3}
0.540 ± 0.01	0.000	
Total bremsstrahlung energy, Mev/beta particle	9.924×10^{-4}	

Bremsstrahlung energy group, Mev	Within ΔE energy group: Photons per beta particle	Within ΔE energy group: Photons w^{-1} sec^{-1}
0.320 ± 0.01	2.458×10^{-5}	1.35×10^{8}
0.340 ± 0.01	1.609×10^{-5}	0.88×10^{8}
0.360 ± 0.01	1.016×10^{-5}	0.56×10^{8}
0.380 ± 0.01	6.135×10^{-6}	3.37×10^{7}
0.400 ± 0.01	3.491×10^{-6}	1.92×10^{7}
0.420 ± 0.01	1.835×10^{-6}	1.01×10^{7}
0.440 ± 0.01	8.638×10^{-7}	0.48×10^{7}
0.460 ± 0.01	3.456×10^{-7}	1.90×10^{6}
0.480 ± 0.01	1.065×10^{-7}	5.86×10^{5}
0.500 ± 0.01	2.007×10^{-8}	1.10×10^{5}
0.520 ± 0.01	1.000×10^{-9}	5.50×10^{3}
0.540 ± 0.01	0.000	
Total bremsstrahlung energy, Mev/beta particle	1.411×10^{-3}	

STRONTIUM TITANATE (Cont'd.)

(2) Photons produced from ^{90}Y beta in $^{90}SrTiO_3$ matrix

Bremsstrahlung energy group, Mev	Within ΔE energy group	
	Photons per beta particle	Photons w^{-1} sec^{-1}
0.100 ± 0.05	4.537×10^{-2}	2.50×10^{11}
0.200 ± 0.05	1.782×10^{-2}	0.98×10^{11}
0.300 ± 0.05	9.456×10^{-3}	5.20×10^{10}
0.400 ± 0.05	5.665×10^{-3}	3.12×10^{10}
0.500 ± 0.05	3.613×10^{-3}	1.99×10^{10}
0.600 ± 0.05	2.389×10^{-3}	1.31×10^{10}
0.700 ± 0.05	1.611×10^{-3}	0.89×10^{10}
0.800 ± 0.05	1.098×10^{-3}	6.04×10^{9}
0.900 ± 0.05	7.493×10^{-4}	4.12×10^{9}
1.000 ± 0.05	5.092×10^{-4}	2.80×10^{9}
1.100 ± 0.05	3.425×10^{-4}	1.88×10^{9}
1.200 ± 0.05	2.264×10^{-4}	1.25×10^{9}
1.300 ± 0.05	1.460×10^{-4}	8.03×10^{8}
1.400 ± 0.05	9.110×10^{-5}	5.01×10^{8}
1.500 ± 0.05	5.434×10^{-5}	3.00×10^{8}
1.600 ± 0.05	3.050×10^{-5}	1.68×10^{8}
1.700 ± 0.05	1.576×10^{-5}	8.67×10^{7}
1.800 ± 0.05	7.220×10^{-6}	3.97×10^{7}
1.900 ± 0.05	2.764×10^{-6}	1.52×10^{7}
2.000 ± 0.05	7.850×10^{-7}	4.32×10^{6}
2.100 ± 0.05	1.239×10^{-7}	6.81×10^{5}
2.200 ± 0.05	3.540×10^{-9}	1.95×10^{4}

Total bremsstrahlung energy, Mev/beta particle 2.078×10^{-2}

STRONTIUM OXIDE (Cont'd.)

Bremsstrahlung energy group, Mev	Within ΔE energy group	
	Photons per beta particle	Photons w^{-1} sec^{-1}
0.100 ± 0.05	6.152×10^{-2}	3.38×10^{11}
0.200 ± 0.05	2.415×10^{-2}	1.33×10^{11}
0.300 ± 0.05	1.281×10^{-2}	0.70×10^{11}
0.400 ± 0.05	7.674×10^{-3}	4.22×10^{10}
0.500 ± 0.05	4.894×10^{-3}	2.69×10^{10}
0.600 ± 0.05	3.234×10^{-3}	1.78×10^{10}
0.700 ± 0.05	2.181×10^{-3}	1.20×10^{10}
0.800 ± 0.05	1.485×10^{-3}	8.17×10^{9}
0.900 ± 0.05	1.014×10^{-3}	5.58×10^{9}
1.000 ± 0.05	6.887×10^{-4}	3.79×10^{9}
1.100 ± 0.05	4.630×10^{-4}	2.55×10^{9}
1.200 ± 0.05	3.000×10^{-4}	1.65×10^{9}
1.300 ± 0.05	1.973×10^{-4}	1.09×10^{9}
1.400 ± 0.05	1.231×10^{-4}	0.68×10^{9}
1.500 ± 0.05	7.337×10^{-5}	4.04×10^{8}
1.600 ± 0.05	4.117×10^{-5}	2.26×10^{8}
1.700 ± 0.05	2.125×10^{-5}	1.17×10^{8}
1.800 ± 0.05	9.740×10^{-6}	5.36×10^{7}
1.900 ± 0.05	3.728×10^{-6}	2.05×10^{7}
2.000 ± 0.05	1.058×10^{-6}	5.82×10^{6}
2.100 ± 0.05	1.670×10^{-7}	9.19×10^{5}
2.200 ± 0.05	4.768×10^{-9}	2.62×10^{4}

Total bremsstrahlung energy, Mev/beta particle 2.814×10^{-2}

STRONTIUM TITANATE (Cont'd.)

B.2.4 Compatibility with Containment Materials

Container Material	Maximum Penetration, mils 168 hr	500 hr	1000 hr
		1000°C	
Haynes 25	Traces	0.1	0.2
Molybdenum	No attack	No attack	No attack
Nionel	1.5	1.7	2.0
Tungsten	Traces	0.2	1.5
TZM	No attack	No attack	No attack
		1850°C	
Molybdenum	No attack	No attack	No attack
Niobium	No attack	--	No attack
Tantalum	No attack	Traces	3.0
Tungsten	No attack	--	No attack
TZM	No attack	Traces	5.0

More data are available in ORNL-4205, Sept. 30, 1967 (Confidential) and ORNL-4237, December 31, 1967 (Confidential)

B.2.5 Thermophysical Properties

a. Density

5.11 g/cm^3 - density of pure $SrTiO_3$
5.03 g/cm^3 - density of average $SrTiO_3$

b. Coefficient of thermal expansion

$\alpha = 11.2 \times 10^{-6}/°C$ (100-700°C)
Data on inactive $SrTiO_3$ have been obtained up to 1400°C. Such data are reported in ORNL-4045, Sep. 30, 1966 (Conf.)

c. Specific Heat and enthalpy

(1) Specific heat in cal $g^{-1}\ °C^{-1}$
$0.154 + 1.11 \times 10^{-5}\ T - 2.49 \times 10^3\ T^{-2}$
(T is in °K)

(2) Enthalpy in calories/mole
$H_T - H_{298} = 28.23\ T + 0.88 \times 10^{-3}\ T^2 + 4.66 \times 10^5\ T^{-1} - 10{,}058$
(T is in °K)

STRONTIUM OXIDE (Cont'd.)

Classified: See USAEC Reports No. ORNL-4189, June 30, 1967 (Confidential) and ORNL-4205, Sept. 30, 1967 (Confidential)

a. Density

4.7 g/cm^3 - density of pure SrO
4.63 g/cm^3 - density of average SrO

b. Coefficient of thermal expansion

$13.92 \times 10^{-6}/°C$ (20-1200°C)
Data up to 1400°C are reported in ORNL-4045, Sep. 30, 1966 (Conf.)

c. Specific heat and enthalpy

(1) Specific heat in cal $g^{-1}\ °C^{-1}$
$0.117 + (1.22 \times 10^{-5}\ T) - (1.50 \times 10^3\ T^{-2})$
(T is in °K)

(2) Enthalpy in calories/mole
$H_T - H_{298} = 12.13\ T + (0.03 \times 10^{-3}\ T^2) + (1.55 \times 10^5\ T^{-1}) - 4192$
(T is in °K)

STRONTIUM TITANATE (Cont'd.)

d. Temperatures of phase transformations

(1) Melting point - 1910°C
(2) Boiling point - 2500-3000°C

e. Latent heats of phase transformations

ΔH fusion (not available)
ΔH vaporization 71 kcal/mole
(calculated from Trouton's rule)

f. Vapor pressure

g. Thermal conductivity

(1) $SrO:TiO_2 = 1.00$

The following equation was derived from data by a method of least mean squares. The data covered the range 350 to 900°C. Useful range of equation is 200 to 1400°C.

$1/k = 55.76 + 0.0673T$ °K cal cm^{-1} sec^{-1} $°C^{-1}$

Temperature, °C	Thermal conductivity,* cal cm^{-1} sec^{-1} $°C^{-1}$
200	0.0114 ± 0.0015
400	0.0099 ± 0.0003
600	0.0088 ± 0.0001
800	0.0078 ± 0.0001
1000	0.0071 ± 0.0002
1200	0.0065 ± 0.0003
1400	0.0060 ± 0.0003

*Determined on theoretically dense pellets of stoichiometric $SrTiO_3$ with a composition of 51.03 wt % SrO, 1.92 wt % BaO, 2.42 wt % CaO, 0.28 wt % MgO, and 44.35 wt % TiO_2 simulating a freshly prepared Hanford product. More data are available in ORNL-4045, Sep. 30, 1966 (Conf.) and ORNL-4084, Dec. 31, 1966 (Conf.). Data on thermal conductivities of $SrTiO_3$ with excess TiO_2 available in ORNL-4131, March 31, 1967 (Conf.).

STRONTIUM OXIDE (Cont'd.)

d. Temperatures of phase transformations

(1) Melting point - 2457°C
(2) Boiling point - 3227°C

e. Latent heats of phase transformations

ΔH fusion 16.7 kcal/mole
ΔH vaporization (not available)

f. Vapor pressure

$\log P = 3.07 \times 10^4 T^{-1} + 13.12$
(T is in °K and P is in atm)

g. Thermal conductivity

(1) SrO = 100%

The following equation was derived from data by a method of least mean squares. The data covered the range 350 to 900°C. Useful range of equation is 200 to 1400°C.

$1/k = 109.51 + 0.0916T$ °K cal cm^{-1} sec^{-1} $°C^{-1}$

Temperature, °C	Thermal conductivity,* cal cm^{-1} sec^{-1} $°C^{-1}$
200	0.0066 ± 0.0006
400	0.0058 ± 0.0003
600	0.0053 ± 0.0001
800	0.0048 ± 0.0002
1000	0.0044 ± 0.0003
1200	0.0041 ± 0.0004
1400	0.0038 ± 0.0004

*Determined on theoretically dense pellets of SrO with a composition of 91.69 wt % SrO, 3.46 wt % BaO, 4.34 wt % CaO, and 0.51 wt % MgO simulating a freshly prepared Hanford product. More data are available in ORNL-4131, March 31, 1967 (Conf.).

STRONTIUM TITANATE (Cont'd.)

(2) Thermal conductivity of various SrO-TiO_2 compositions

See Figure B-5

h. Thermal diffusivity

Temperature, °C	Thermal diffusivity,* cm^2/sec
200	0.0151
400	0.0124
600	0.0107
800	0.0093
1000	0.0083
1200	0.0075
1400	0.0068

*Calculated by dividing the thermal conductivity by the product of the specific heat and the density.

i. Viscosity: Not available

j. Surface tension: Not available

k. Total hemispherical emittance: Not available

l. Spectral emissivity: Not available

m. Crystallography

Cubic: a = 3.899 kX

STRONTIUM OXIDE (Cont'd.)

(2) Thermal conductivity of various SrO-TiO_2 compositions

See Figure B-5

h. Thermal diffusivity

Temperature, °C	Thermal diffusivity,* cm^2/sec
200	0.0122
400	0.0103
600	0.0091
800	0.0080
1000	0.0072
1200	0.0066
1400	0.0060

*Calculated by dividing the thermal conductivity by the product of the specific heat and the density.

i. Viscosity: Not available

j. Surface tension: (Determined for MgO)
1200 dyn/cm

k. Total hemispherical emittance: Not available

l. Spectral emissivity: (Determined for BeO)

Total emissivity	Temperature, °C
0.36	1000
0.46	1400
0.50	1800

Small amounts of impurities such as carbon or radiation darkening can increase these values significantly to ~ 0.9.

m. Crystallography

Cubic - face centered:
a = 5.1396 kX

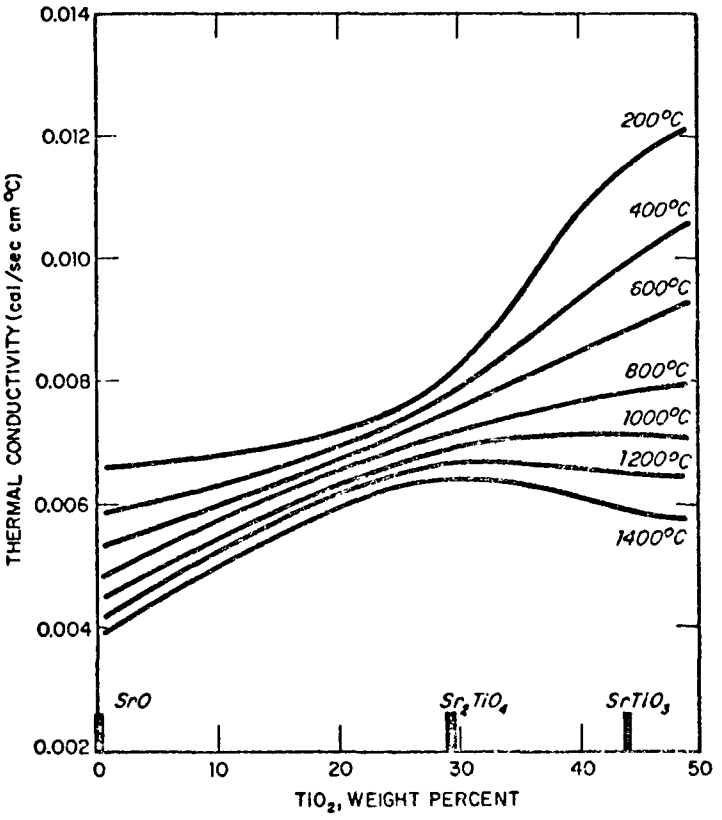

Figure B-5. Thermal Conductivity of Various SrO-TiO_2 Compositions. Obtained by interpolating the data for stoichiometric SrO, Sr_2TiO_4, $SrTiO_3$ and TiO_2.

STRONTIUM TITANATE (Cont'd)

B.2.6 Solubilities

See Figure B-6

B.2.7 Mechanical Properties

a. Hardness: Not available

b. Crush strength: (Determined on $CeTiO_3$) 19,100 lb/in^2

c. Bend strength: 43 lb/in^2

B.2.8 Chemical Properties

a. Heat and free energy of formation, entropy

(1) Heat of formation

ΔH°_f = -399 kcal/mole
(calculated from available data)

(2) Free energy of formation

ΔF°_f = -379 kcal/mole
(calculated from available data)

(3) Entropy

S°_{298} = 26.0 eu

STRONTIUM OXIDE (Cont'd)

Reacts with water or HCl and dissolves. The leach rates were determined for SrO using ^{85}Sr tracer. Values were obtained for a 24-hour period in static distilled water. The average of six values is 1.35 ± 0.38 g cm^{-2} day^{-1} (confidence limit at 95% level). The leach rate determined by weight loss measurement of 44-g samples in flowing distilled water (4.4 cm/min) was 1.49 g cm^{-2} day^{-1}. Leached SrO appeared to be completely in an ionic form.* Solutions passed in millipore filter (0-1μ) left no deposite. Data on dissolution rates of SrO pellets are available in ORNL-4131, 31 March 1967 (CONFIDENTIAL).

a. Hardness: 3.5 mohs

b. Crush strength: Not available

c. Bend strength: Not available

a. Heat and free energy of formation, entropy

(1) Heat of formation

ΔH°_f = -141.0 kcal/mole

(2) Free energy of formation

ΔF°_f = -133.8 kcal/mole

(3) Entropy

S°_{298} = 13.0 eu

* McHenry, R. E., ORNL, Personal Communication, August 1967.

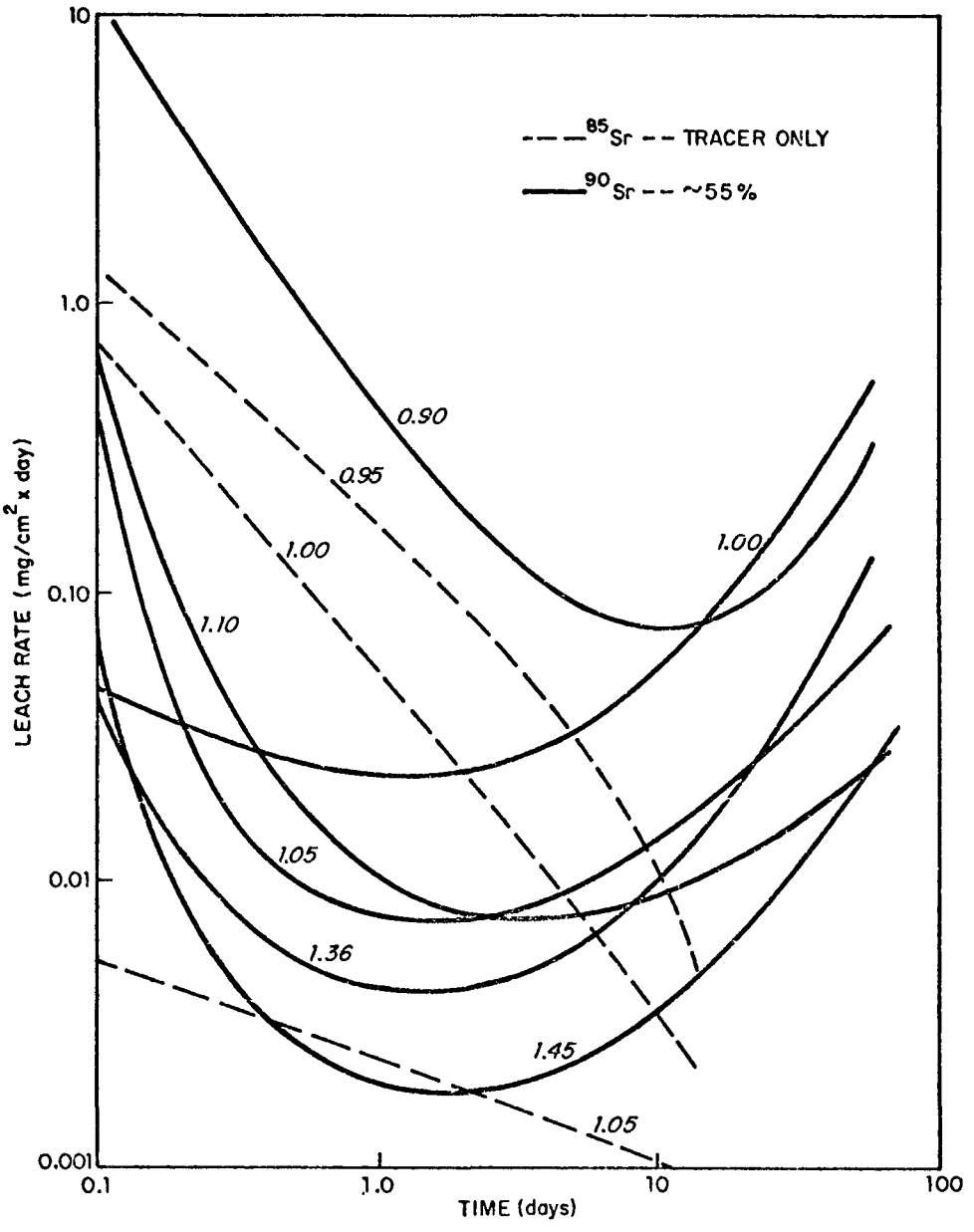

Figure B-6. Leach Rates of $SrTiO_3$ in Distilled Water for TiO_2/SrO Ratios of 0.90 to 1.45

STRONTIUM TITANATE (Cont'd.)

b. Chemical reactions and reaction rates (oxygen, nitrogen, water, steam, hydrogen, liquid metals, other)

(1) Oxygen - no reaction
(2) Nitrogen - no reaction
(3) Water - decomposes
(4) Inorganic acids - soluble

B.2.9 Biological Tolerances

Same as listed in Table I, Section B.1.9

B.2.10 Shielding

Figures B-7 to B-10 present the Bremsstrahlung dose rates from ^{90}Sr power sources of 100, 200, 500, 1000, 2000, 5000, 10,000, and 20,000 watts with iron, lead, and uranium shielding.

STRONTIUM OXIDE (Cont'd.)

b. Chemical reactions and reaction rates (oxygen, nitrogen, water, steam, hydrogen, liquid metals, other)

(1) Oxygen - no reaction
(2) Nitrogen - no reaction
(3) Water - forms $Sr(OH)_2$
(4) Inorganic acids - soluble
(5) CO_2 - reacts to form $SrCO_3$

Same as listed in Table I, Section B.1.9

Figures B-11 to B-14 present the Bremsstrahlung dose rates from ^{90}Sr power sources of 100, 200, 500, 1000, 2000, 5000, 10,000, and 20,000 watts with iron, lead, and uranium shielding.

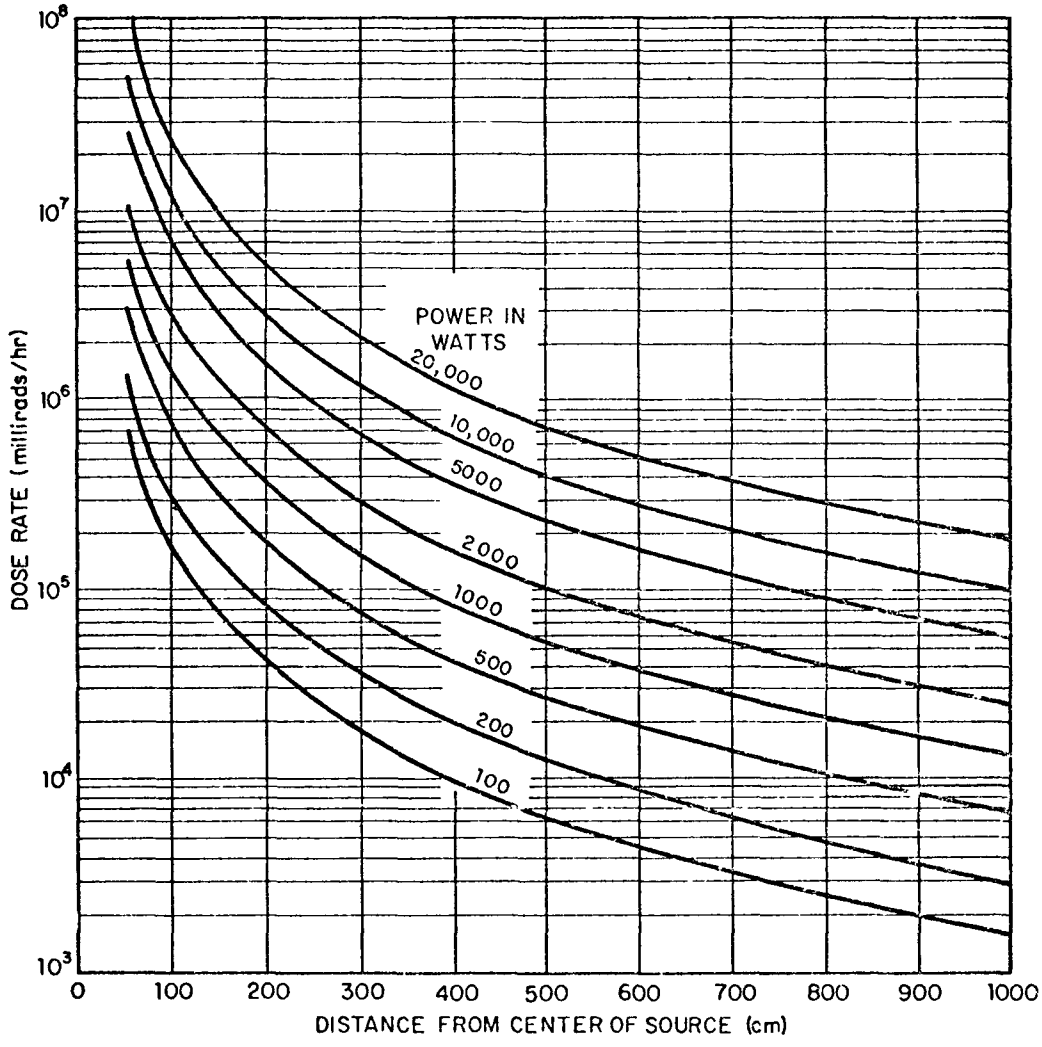

Figure B-7. Bremsstrahlung Dose Rates from Unshielded Isotopic Power Sources of Strontium-90 Titanate as a Function of Distance from Center of Source

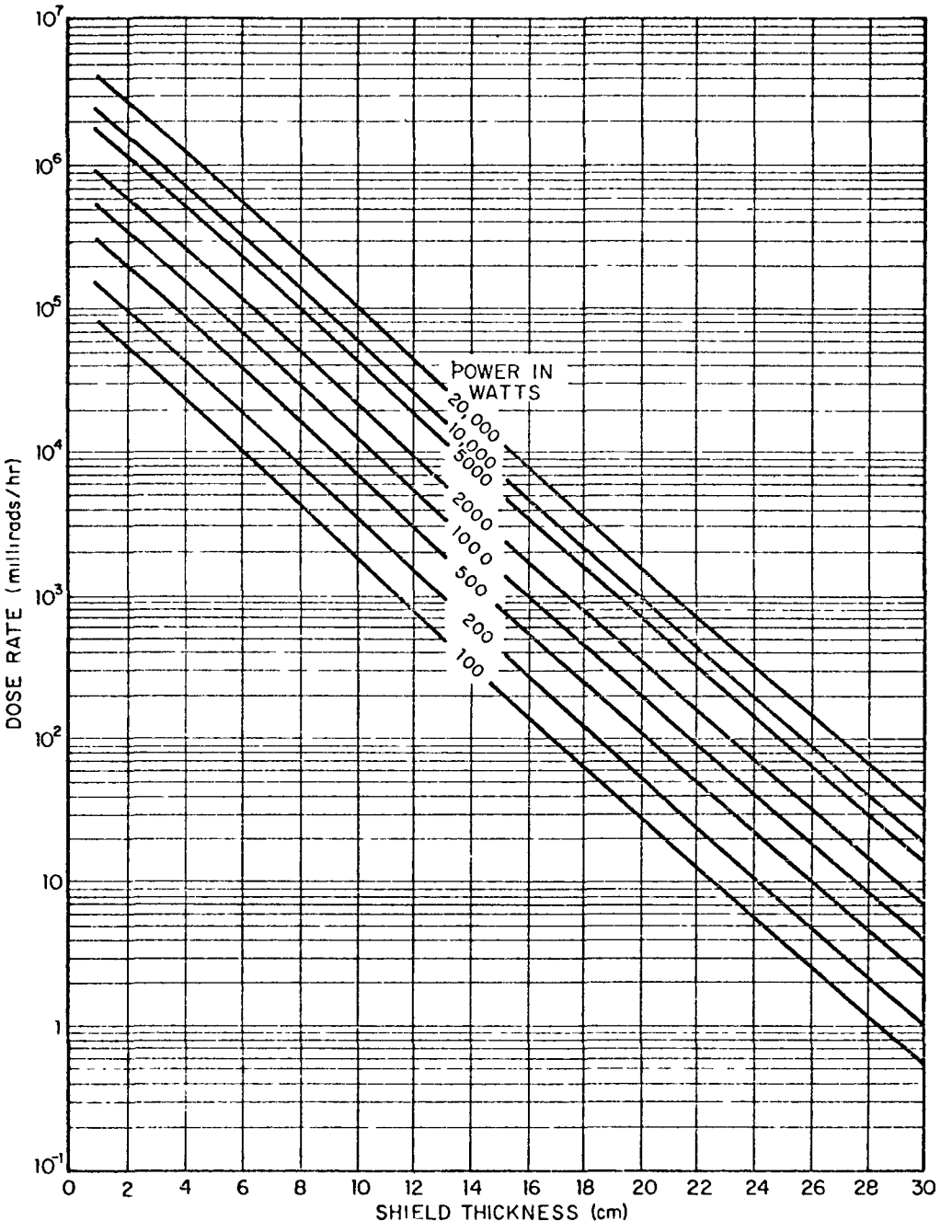

Figure B-8. Bremsstrahlung Dose Rates from Iron-Shielded Isotopic Power Sources of Strontium-90 Titanate. Center of source to dose point separation distance = 100 cm.

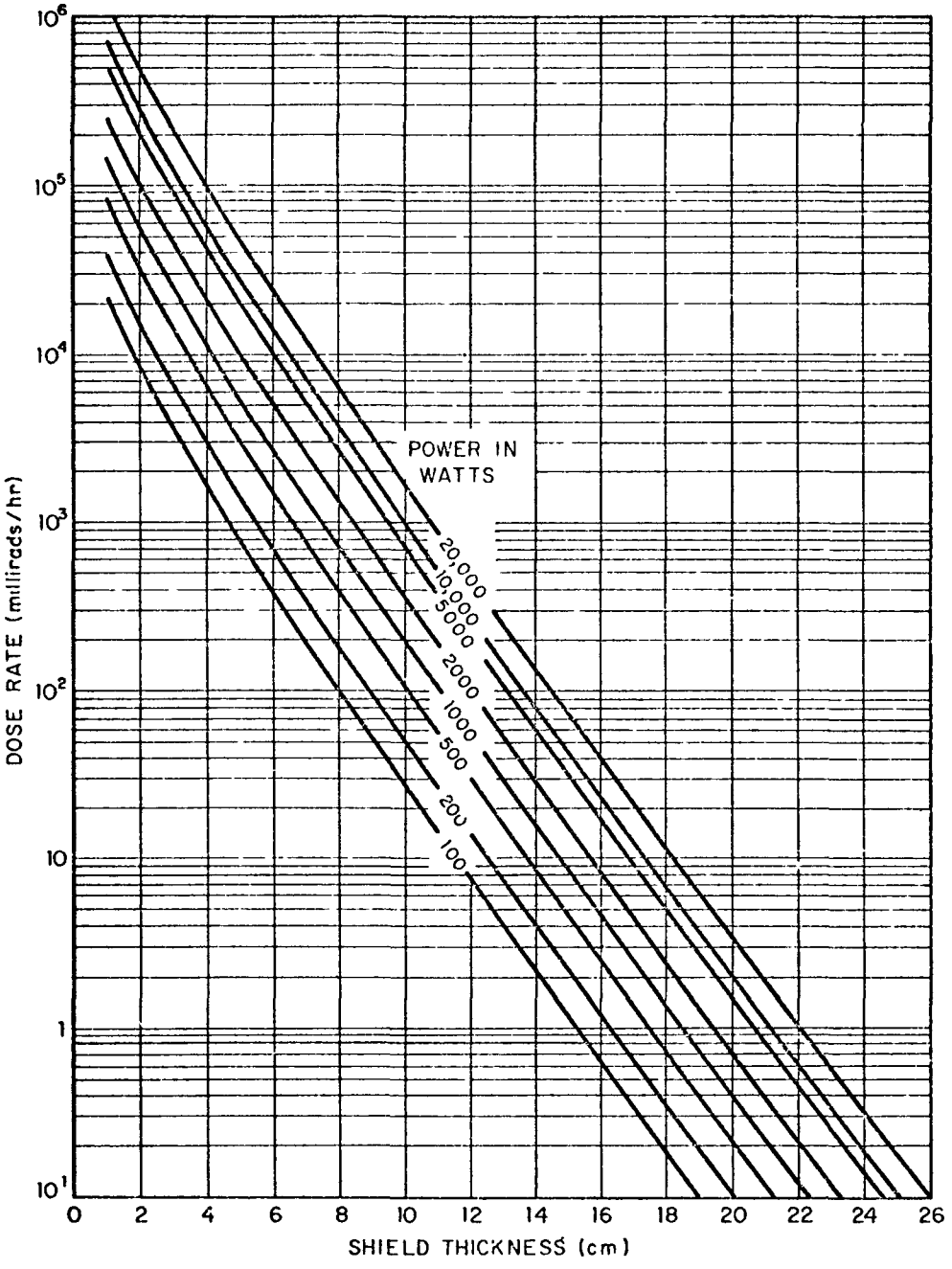

Figure B-9. Bremsstrahlung Dose Rates from Lead-Shielded Isotopic Power Sources of Strontium-90 Titanate. Center of source to dose point separation distance = 100 cm.

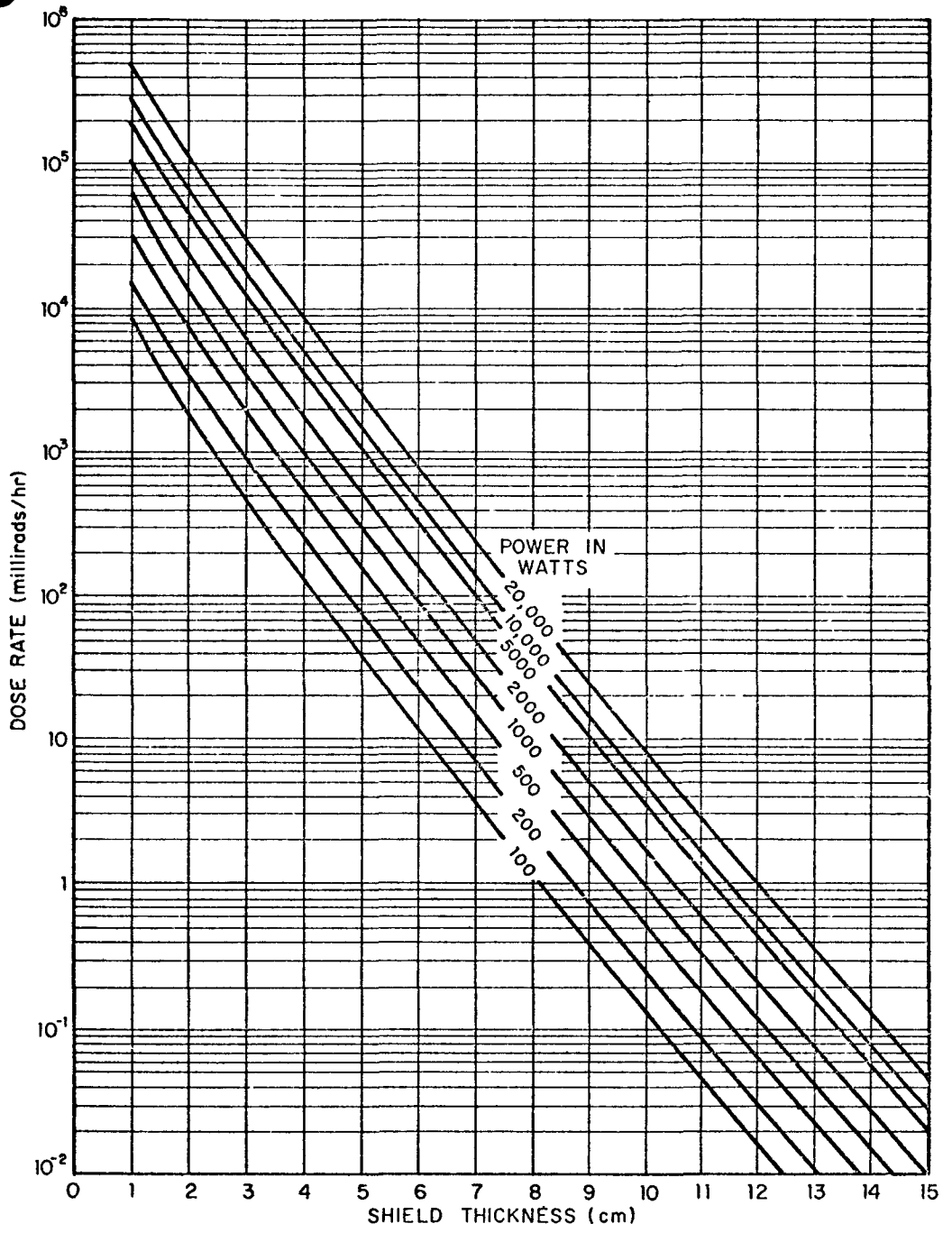

Figure B-10. Bremsstrahlung Dose Rates from Uranium-Shielded Isotopic Power Sources of Strontium-90 Titanate. Center of source to dose point separation distance = 100 cm.

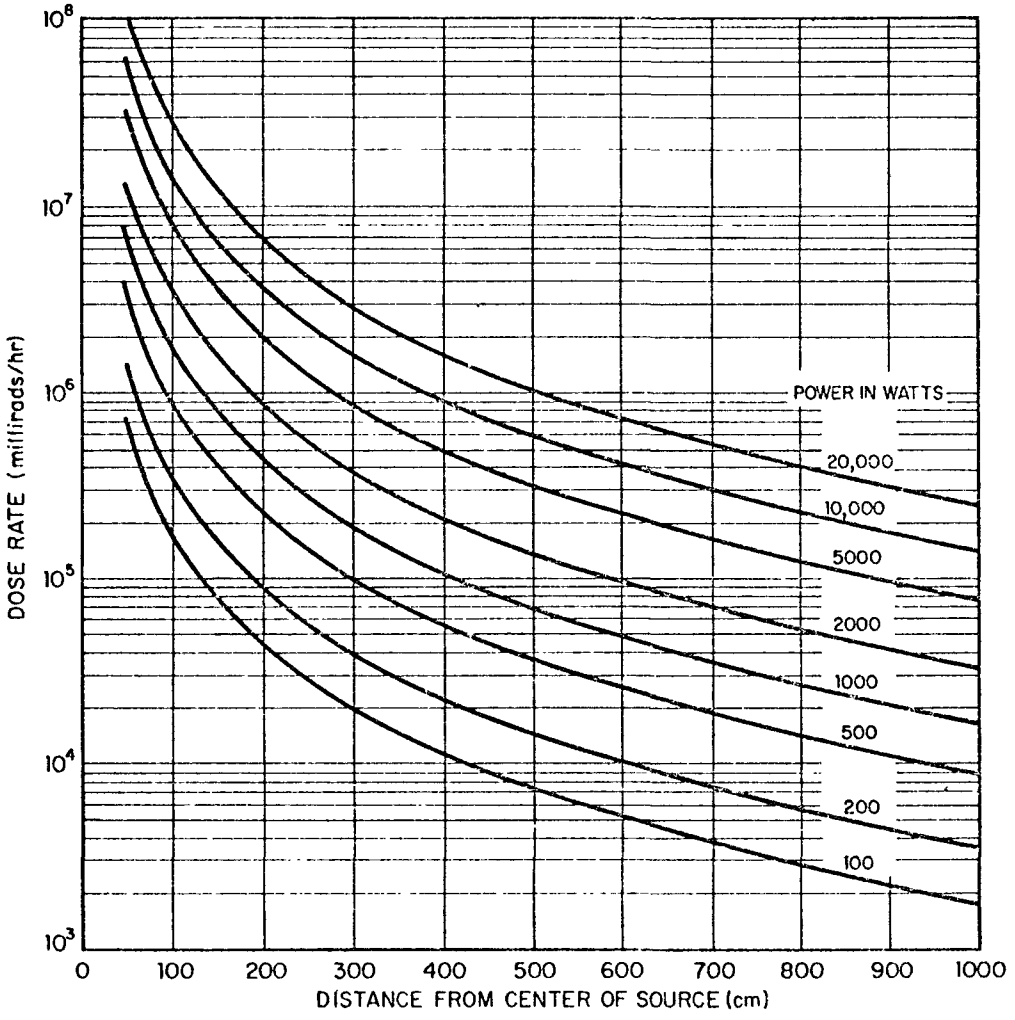

Figure B-11. Bremsstrahlung Dose Rates from Unshielded Isotopic Power Sources of Strontium-90 Oxide as a Function of Distance from Center of Source.

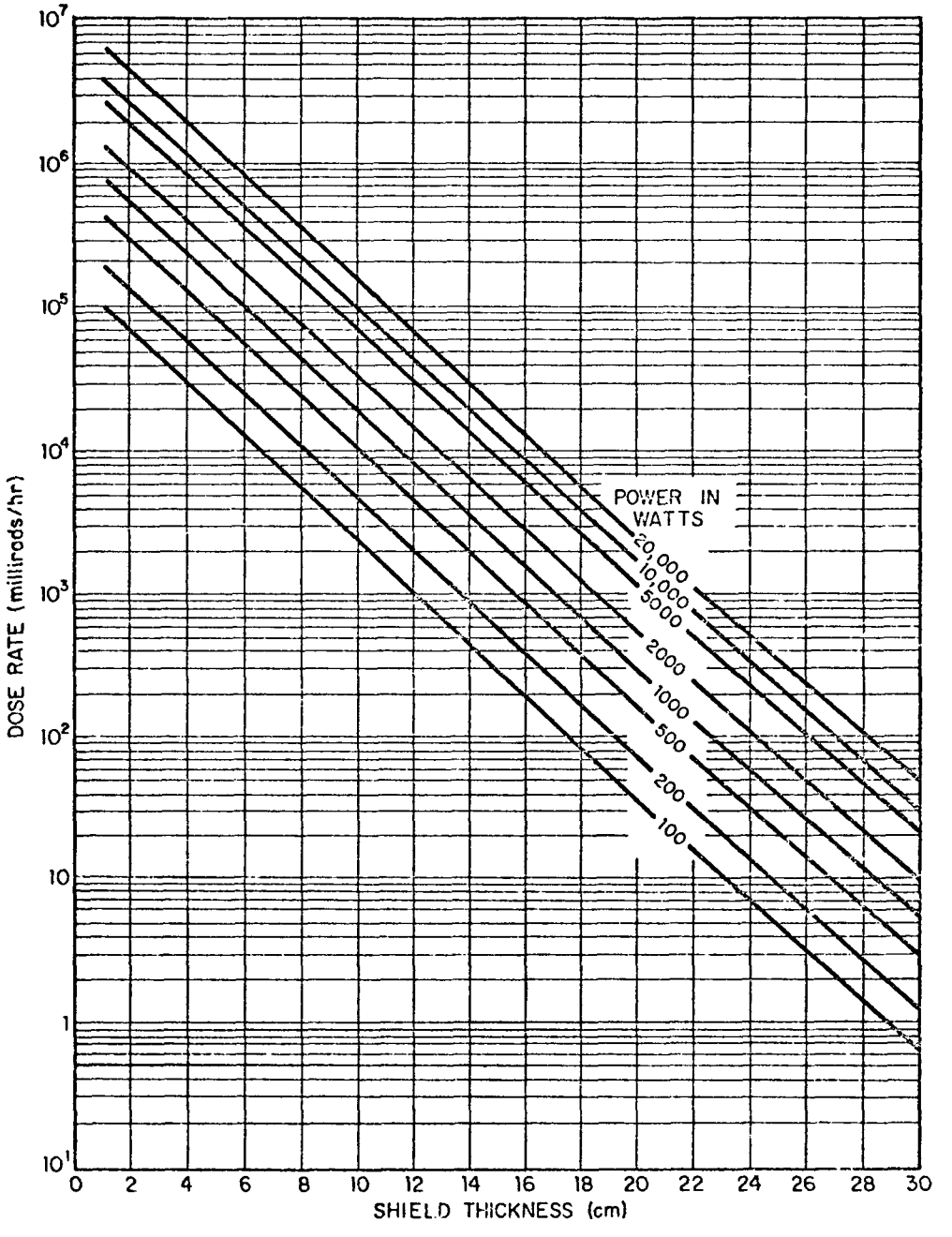

Figure B-12. Bremsstrahlung Dose Rates from Iron-Shielded Isotopic Power Sources of Strontium-90 Oxide. Center of source to dose point separation distance = 100 cm.

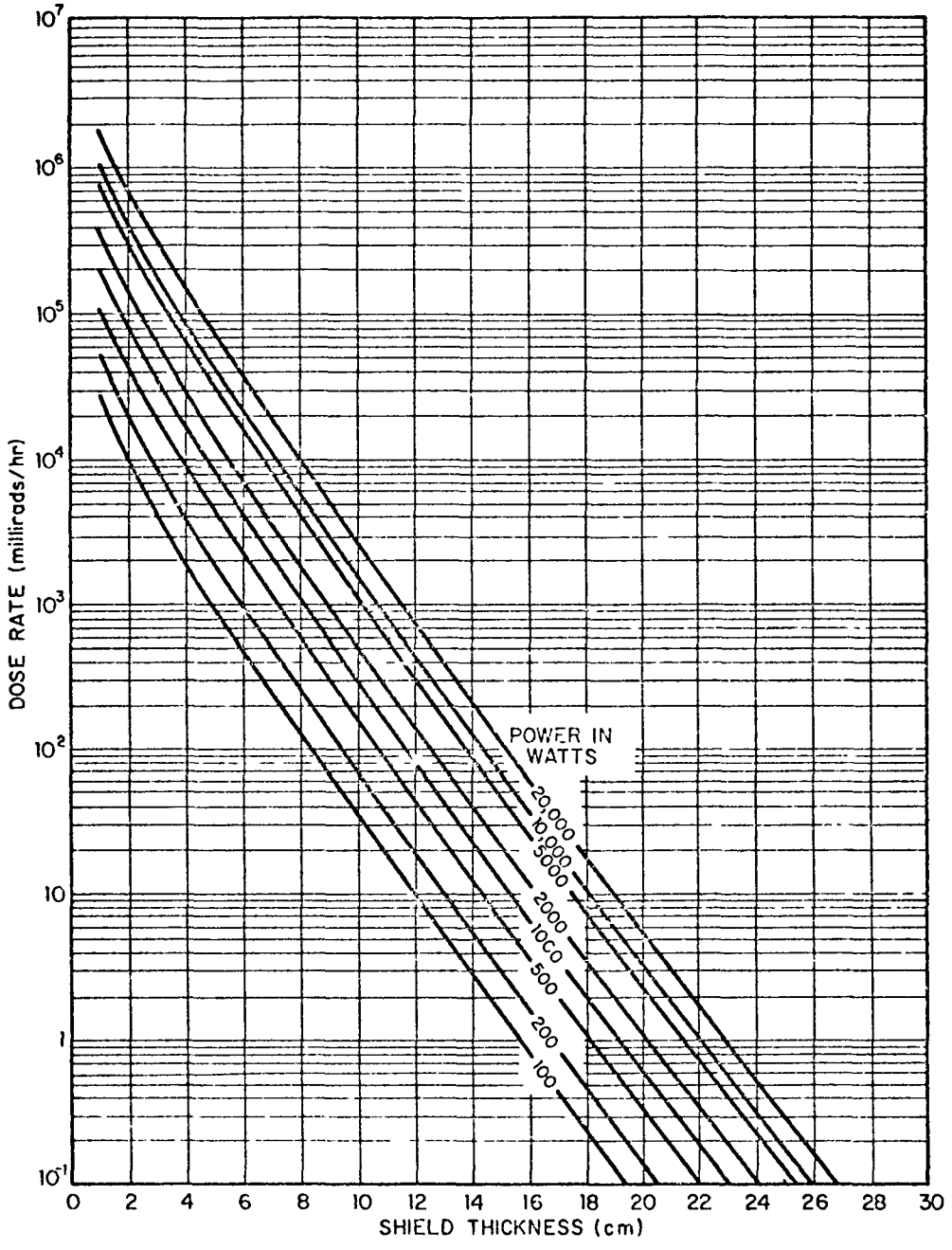

Figure B-13. Bremsstrahlung Dose Rates from Lead-Shielded Isotopic Power Sources of Strontium-90 Oxide. Center of source to dose point separation distance = 100 cm.

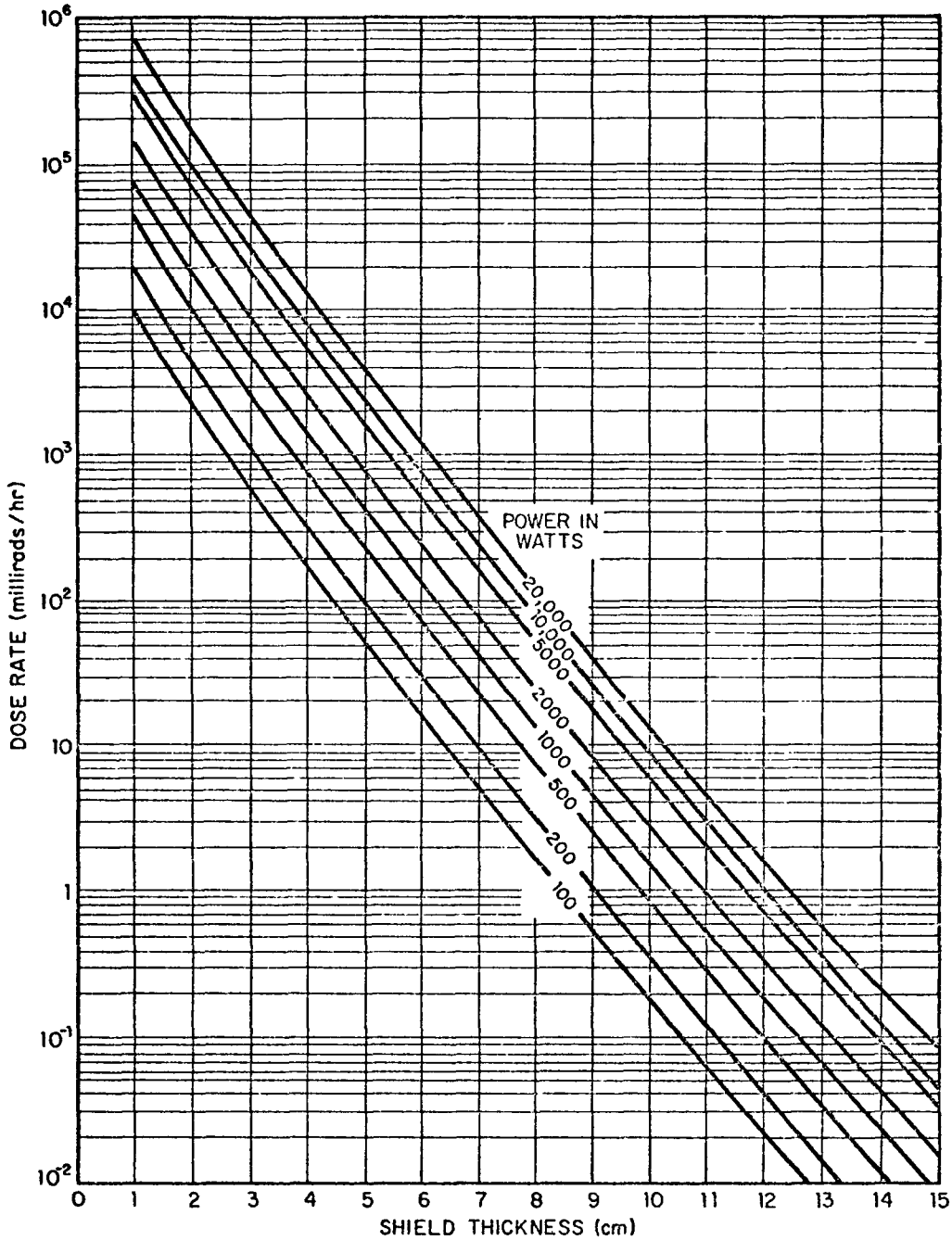

Figure B-14. Bremsstrahlung Dose Rates from Uranium-Shielded Isotopic Power Source of Strontium-90 Oxide. Center of source to dose point separation distance = 100 cm.